Taras Shevchenko National University of Kyiv
Astronomical Observatory

Astronomy and Space Physics in the Kyiv University

Book of Abstracts

International Conference
in part of the Science Day in Ukraine

May 28 – May 31, 2024

Kyiv, Ukraine

ASTRONOMY AND SPACE PHYSICS IN KYIV UNIVERSITY

Scientific organizing committee (SOC)

Chair: Vasyl' Ivchenko (Ukraine)
Co-chair: Volodymyr Efimenko (Ukraine

SOC Secretary I. Lyk'yanyk (Ukraine)

SOC Members
Artem Bohdan (Germany), Oleksandra Ivanova (Slovakia), Liliya Kazantseva (Ukraine), Vsevolod Lozitsky (Ukraine), Gennadi Milinevsky (Ukraine), Sergiy Parnovsky (Ukraine), Oleh Petruk (Italy), Vira Rosenbush (Ukraine), Yaroslav Yatskiv (Ukraine), Vasyl' Yurchyshyn (USA), Valentyna Zharkova (UK), Valery Zhdanov (Ukraine)

Local organizing committee (LOC)

Chair V. Efimenko (Ukraine)
Secretary: Alena Mozgova (Ukraine)

LOC Members
Vassyl Danylevsky, Asen Grytsai, Anatoly Tugay, Ivan Yakovkin, Svitlana Zaychenko

E-mail: aoconf@ukr.net

Place of the meeting (Web-conference on zoom-platform) Astronomical observatory of the Taras Shevchenko national university of Kyiv, Observatorna str., 3

CONTENTS

ASTRONOMY AND SPACE PHYSICS IN KYIV UNIVERSITY

ASTRONOMY AND SPACE PHYSICS IN KYIV UNIVERSITY

ASTRONOMY AND SPACE PHYSICS IN KYIV UNIVERSITY

ASTRONOMY AND SPACE PHYSICS IN KYIV UNIVERSITY

PLENARY SESSIONS

Self-consistent equilibrium of a force-free magnetic flux rope

Oleg K. Cheremnykh[1] and Volodymyr M. Lashkin[2,1]

[1] Space Research Institute, Glushkov Ave 40, 4/1, 03680, Kyiv 187, Ukraine
[2] Institute for Nuclear Research, Pr. Nauky 47, Kyiv 03028, Ukraine

We have obtained the integral equilibrium equation for a cylindrically symmetric force-free magnetic flux rope. Using this equation, a new local relationship between the axial magnetic field strength and electric current density was found and a nonlinear equation for the axial current density was derived. We have found an analytical solution to this equation, which made it possible to completely solve the problem of finding a self-consistent equilibrium of the force-free magnetic flux rope. We have obtained exact analytical expressions for the self-consistent components of the electric current density and magnetic field. It is shown that all equilibrium quantities are determined by the total axial current and the maximum density of this current. It was established that the found magnetic field qualitatively coincides with the Gold-Hoyle magnetic field. However, unlike the Gold-Hoyle solution, in the solution we obtained, the twist of the magnetic field lines is not an arbitrary value, but is determined by the axial current

Energetics of physical processes during the geospace storm on April 23–24, 2023

L.F. Chernogor

V.N. Karazin Kharkiv National University, Kharkiv, Ukraine

Studying and forecasting the state of space weather is an important interdisciplinary and applied problem. The main cause of variations in space weather are solar storms and their consequences, geospace storms. A geospace storm is synergistically interacting storms in the magnetosphere, ionosphere, atmosphere, and the electric field of atmospheric-ionospheric-magnetospheric origin. The study of the entire variety of physical effects accompanying geospace storms remains an urgent scientific and applied problem today. Each geospace storm, in addition to general patterns, has individual features. Manifestations of geospace storms depend on the specifics of the solar storm, position in the solar cycle, time of year, time of

day, geographic coordinates of the observation site, etc. Manifestations of geospace storms depend on the research method and means of observation. In recent years (since 2019) they have been characterized by high solar activity. On April 23–24, 2023, one of the three strongest geospace storms in the 25th solar cycle took place. An important task is a detailed study of the features of this unique storm. One of the manifestations of the uniqueness of the storm was that the aurora was observed in a number of regions of Ukraine.

The purpose of the work is to assess the energy parameters of the geospace storm in all subsystems of the Sun – interplanetary medium – magnetosphere – ionosphere – atmosphere – Earth (inner shells) system.

On April 21, 2023, an M1.77 class flare occurred on the Sun. As a result of a solar storm that day, a coronal mass ejection took place. The disturbed solar wind reached the Earth's magnetosphere on April 23, 2023 and caused a geospace storm. The main feature of the geospace storm on April 23–24, 2023, and therefore its components, was that the storm was recurrent. This fact once again indicates that each geospace storm has its own unique characteristic features.

Solar storm energetics. The flare began at 17:57 UT and ended at 18:45 UT. The radiation maximum was recorded at 18:12 UT. The total duration of the flare was about 4 hours. With an energy flux density of $1.77 \cdot 10^{-5}$ W/m^2, we have a flare power near the Earth of $2.26 \cdot 10^9$ W and an energy of about $1.6 \cdot 10^{15}$ J. The total flare power was $2.5 \cdot 10^{18}$ W, and its energy was $1.8 \cdot 10^{22}$ J. Along with the solar flare, a coronal mass ejection took place, which near the Earth had a speed of up to 706 km/s, a particle number density of up to $2.1 \cdot 10^7$ м$^{-3}$ and a plasma density of $3.6 \cdot 10^{-20}$ kg/m^3. The plasma temperature reached $2.05 \cdot 10^6$ K. The solar storm was accompanied by the injection of solar cosmic rays with a proton flux density of $3.3 \cdot 10^6$ m^{-2}s^{-1} and a duration of about 4 hours. This ray flux had a maximum value at 18:20 UT on April 23, 2023. This particle flux density value corresponds to the energy flux density of protons with an energy of no less than 10 MeV $5.3 \cdot 10^{-4}$ W/m^2. The power and energy of solar cosmic rays were $6.8 \cdot 10^{10}$ W and $4.9 \cdot 10^{14}$ J.

Magnetospheric storm energetics. The disturbed solar wind, having reached the magnetosphere, led to the onset of a magnetospheric storm. The energy of the magnetospheric storm is described by the Akasofu's epsilon parameter, the spikes of which did not exceed 220 and 160 GJ/s. In addition to the influence of magnetic pressure, the Earth's magnetosphere was affected by dynamic pressure with a power of $4.9 \cdot 10^{11}$ W. For a duration of 10 hours we have an energy of $1.8 \cdot 10^{16}$ J. The power of thermal pressure did not exceed $2.7 \cdot 10^{10}$ W. The Akasofu's epsilon parameter also

determines the energy of a geospace storm. In order to quantitatively characterize geospace storms and to perform their classification, the author introduced a special index equal to 13.4 and 12.0 dB. Both geospace storms was classified as moderate storms. They correspond to energies of about 11 and 4 PJ.

Magnetic storm energetics. It is assessed according to the D_{st}-index values. For the first and second magnetic storms, the energy was 8.1 and 9.7 PJ. According to the NOAA classification, these storms correspond to G4 index, that is, severe. According to the author's classification, these storms were more than severe. The power of the storms was close to 173 and 674 GW.

Ionospheric storm energetics. In this case, both storms were negative. For the qualitative and quantitative characteristics of ionospheric storms, the author introduced a special index, which was 7.6 (the storm is severe) and 4.1 (the storm is strong). Negative ionospheric storms were accompanied by an increase in electron temperature and ion temperature by approximately 100–110%. This led to a loss of ionospheric thermal energy by –1.1 and –0.26 TJ. The ionospheric storms lasted about 20 and 8 h. The average thermal power was about 15.3 and 9 MW. The energy of disturbed dynamic processes in the ionosphere was much less than the energy of thermal processes. During geospace storms, the strength of the ionospheric-magnetospheric electric field with an energy of 20–200 kJ increased by 1–2 orders of magnitude.

Atmospheric storm energetics. A geospace storm is accompanied by a disturbance of the neutral particles number density in the upper atmosphere, the chemical composition of the atmosphere, the generation of acoustic-gravity waves (AGWs) directed from the poles to the equator, an increase in the electric field strength near the atmospheric surface layer, etc. The thermal process caused by an increase in particle number density has the greatest energy. The increase in atmospheric thermal energy reached 108 TJ, while the average power was 3 GW. The increase in atmospheric electric field energy did not exceed 138 GJ, and the average power reached 57.5 MW.

Aurora borealis energetics. An increase in solar wind power led to the generation of aurora on the night of April 23–24, 2023, with a flux density of $9.8 \cdot 10^{-5}$ W/m^2 and an aurora power of $9.8 \cdot 10^8$ W. According to the international scale, this flux value corresponds to coefficient III and an emission intensity of 27.5 kR. The duration of the airglow, depending on the latitude, was 10^2–10^4 s. The aurora energy was 0.1–10 TJ.

The author has improved the international emission intensity scale and added the V coefficient, which describes auroras during extreme geospace storms. An energy scale for auroras has been proposed.

Infrasound energetics. Auroras are accompanied by the generation of infrasound oscillations in the period range of 10–100 s with an amplitude of 0.1–10 Pa. The infrasound power and energy reached 300 MW and 3 TJ.

Earthquake energetics. AGWs generated by auroras are capable of exciting seismic waves with the AGW periods. For acoustic and gravity waves, the earthquake energy did not exceed $8.4 \cdot 10^2$ and $2.8 \cdot 10^5$ J.

Main results. The solar storm on April 21, 2023 caused a powerful geospace storm. As a result, magnetospheric, ionospheric, atmospheric, magnetic and electrical storms were observed on our planet on April 23–24, 2023. The uniqueness of the storm was the occurrence of aurora even in mid-latitudes (up to 50°). The second feature of the storm is associated with its recurrence. The energy characteristics of physical processes, starting from the Sun and ending with the disturbance of the lithosphere, are assessed. A comparative analysis of the parameters of the geospace storm on April 23–24, 2023 and an extreme geospace storm was carried out. The international aurora brightness scale has been improved. An energy scale for auroras has been proposed.

The study was partially supported by State Budget grants provided by the Ministry of Education and Science (registration nos. 0122U001476 and 0124U000478).

Gauge-field production during axion inflation

E.V. Gorbar[1,2], O.O. Sobol[1], S.I. Vilchinskii[1]

[1]Physics Faculty, Taras Shevchenko National University of Kyiv, Kyiv, Ukraine
[2]Bogolyubov Institute for Theoretical Physics, Kyiv, Ukraine

The paradigm of inflation is a very successful idea that not only solves a large number of cosmological problems, but also provides a convincing mechanism for the origin of the primordial perturbations which are the seeds for CMB anisotropies and the modern large-scale structure of the Universe. Therefore, it looks very natural to assume that cosmic inflation may also give rise to primordial magnetic fields which could serve as seeds for magnetic fields in galaxies and galaxy clusters and possibly explain the presence of magnetic fields in voids detected in gamma-ray observations

from distant blazars. Among many possible models of inflationary magnetogenesis one particular model - the axion inflation - where a pseudoscalar inflaton field is coupled to an Abelian gauge field through the Chern-Simons term is quite promising. Despite the fact that this idea originates from the early 1990s, it has attracted a lot of attention in the literature in the last years as it has many phenomenological applications (e.g., to baryogenesis, the production of gravitational waves, primordial black holes etc.). An overview of methods used to describe the gauge-field production, including the gradient expansion method, during axion inflation are given and interesting (potentially observable) features arising in the regime of strong backreaction are discussed.

DART experiment: the impact on Dimorphos and Didymos

Yu. Krugly[1], I. Belskaya, Z. Donchev[3], R. Inasaridze[4,5], V. Ayvazian[4], O. Burkhonov[6], K. Ergashev[6], I. Reva[7], A. Sergeyev[8,1], V. Kouprianov[9], J. Haislip[9], D. Reichart[9], O. Ivanova [10,11,12], I. Lukyanyk[12]

[1]Institute of Astronomy of V. N. Karazin Kharkiv National University, Kharkiv, Ukraine
[2]LESIA, Observatoire de Paris, France
[3]Institute of Astronomy and NAO, Bulgarian Academy of Sciences, Sofia, Bulgaria
[4]E. Kharadze Georgian National Astrophysical Observatory, Abastumani, Georgia
[5]Samtskhe-Javakheti State University, Akhaltsikhe, Georgia
[6]Ulugh Beg Astronomical Institute, Tashkent, Uzbekistan
[7]Fesenkov Astrophysical Institute, Almaty, Kazakhstan
[8]Université Côte d'Azur, Observatoire de la Côte d'Azur, CNRS, Laboratoire Lagrange, Nice, France
[9]University of North Carolina, Chapel Hill, North Carolina, USA
[10]Astronomical Institute of the Slovak Academy of Sciences, Tatranská Lomnica, Slovak Republic
[11]Main Astronomical Observatory of the NASU, Kyiv, Ukraine
[12]Taras Shevchenko National University of Kyiv, Astronomical Observatory, Kyiv, Ukraine

At the end of September 2022, the solution to the international problem of the asteroid hazard has moved to a qualitatively new level. From understanding the number and size of hazardous celestial bodies in the near-

Earth space and the scale of destruction after the fall of such bodies to Earth, the world scientific community obtained the results of the first space experiment on changing the orbit of an asteroid by the method of transferring kinetic momentum (Kinetic Impact). The collision of the DART spacecraft (NASA) with the binary asteroid Didymos showed the effectiveness and feasibility of using Kinetic Impact to change the orbits of asteroids that are hazardous for Earth.

The preparation and carring out of the DART experiment was carried out within the framework of cooperation between the space agencies NASA and ESA. The development of the experiment scheme, registration and analysis of the consequences of the collision was entrusted to the international team of scientists "DART Investigation Team". An important part of the experiment was the organization of observations of the asteroid. A parallel recording of the moment of collision of the DART spacecraft with the Dimorphos satellite of the Didymos binary system was organized using a small observational cubesat the LICIAcube (Light Italian Cubesat for Imaging of Asteroids). Ground-based and space telescopic observations of the asteroid Didymos before and after the DART impact were organized and carried out, which made it possible to determine the consequences of the collision.

Based on the results of ground-based photometric observations, an unexpectedly large period change in the rotation period of the Dimorphos satellite around the main body of the system was determined (a reduction of 33 minutes), which means a change in the parameters of its orbit. The characteristic features of the consequences of the collision were determined: the rapid process of the shock wave, the formation of a dust shell around the binary system, the emergence and long-term existence of a dust tail. The authors of the report carried out photometric and polarimetric observations of the asteroid Didymos almost a month after the moment of collision, at the end of October 2022, which showed albedo changes on the surface of the main body of the binary system.

The report includes details of the preparation, conduct and results of the DART experiment.

Muon tomography: looking inside nuclear reactors

A. Mozgova[1], B. Hnatyk[1], S. Gabielkov[2], E. Zhyhaniuk[1]

[1]Astronomical Observatory of Taras Shevchenko National University of Kyiv, Kyiv, Ukraine
[2]Institute for Safety Problems of Nuclear Power Plants, NAS of Ukraine, Chornobyl, Ukraine

Due to the large number and high penetrating ability of muons of secondary cosmic rays, muon tomography is widely used in engineering, industry, volcanology, archeology for research and analysis of various structures, detection of geological features of volcanoes, etc. Muon tomography does not require artificial sources of probing radiation, which is its significant advantage over other methods of non-destructive testing.

An important area of application of muon tomography is nuclear safety and control over the movement of nuclear materials and in the management of high-level radioactive waste, in particular, analysis of the state of nuclear power reactors, determination of the content and spatial distribution of radioactive substances inside the reactor.

The work reviews the application of muon tomography to the study of the location of nuclear materials in power reactors of nuclear power plants, containers for transporting nuclear materials, etc. The study of the current state of lava-like fuel-containing materials, which were formed during the accident at the 4th unit of the Chornobyl NPP in 1986, is an urgent task. The space of location of radionuclides, fission and activation products, the density of lava-like fuel-containing materials in the rooms of Unit 4 of the ChNPP is proposed to be determined using muon detectors.

21cm cosmology in the first quarter of 21st century: predictions and expectations

B. Novosyadlyj

Astronomical Observatory of Ivan Franko National University of Lviv, Ukraine,
International Center of Future Science, College of Physics of Jilin University, P. R. China

The tensions of ΛCDM model in the interpretations of observational programs of the last years, devoted to study the CMB anisotropy, expansion of the Universe and formation of the large-scale structure, encourage to search the new cosmological tests. Signal in the 21cm hydrogen line from the first billion years Universe predicted by theorists can be one from them. On the other hand, JWST discoveries of massive galaxies and traces of ionized helium at redshifts ~12-13 have heightened interest in the Dark Ages, which preceded the appearance of the first stars and galaxies. A signal in the hyperfine structure line 21cm of neutral hydrogen from the rarefied intergalactic medium and halos, which are forming, can be the main channel of information about state of baryonic matter at that epoch, its ionization, temperature and bulk motions. The aim of the talk is the review of current state of 21cm cosmology, its theoretical predictions, observational possibilities and expectations.

The formation of global signals in the redshifted 21cm hydrogen line, luminosity of halos and power spectrum of fluctuation of brightness temperature will be discussed. Especially, it will be illustrated the dependences of the line profile of global signal on cosmological parameters of ΛCDM model, nature of dark matter particles and type of dark energy in the Dark Ages, Cosmic Dawn, and Reionization epochs. It will be also shown that the position and depth of the Cosmic Dawn line, due to the Wouthuysen-Field effect, is mainly defined by the spectral energy distribution of the first sources of light. So, the tomografy of young Universe can shed the light on the key problems of current cosmology.

The possibility of detecting of the global and interferometric signals at redshifts ~10-100 will be briefly discussed also, as well as the current and future observational facility projects will be mentioned.

ASTRONOMY AND SPACE PHYSICS IN KYIV UNIVERSITY

Magnetic diagnostics of the solar corona using EUV lines

N.G. Shchukina[1,2] and J. Trujillo Bueno[2]

[1]Main Astronomical Observatory of NAS of Ukraine, Kyiv, Ukraine
[2]Instituto de Astrofísica de Canarias, E-38205, La Laguna, Tenerife, Spain
shchukin@mao.kiev.ua ,natasha-ext@iac.es, jtb@iac.es

The aim of our study is to investigate the diagnostic capabilities of linear polarization signals in electric-dipole EUV coronal lines of highly ionized Fe X, Fe XI, Fe XIII and Si IX atoms for coronal magnetic field measurements. We confirm that the mechanism shown in 2009 by Manso Sainz and Trujillo Bueno for the Fe X 174 Å line works also in many EUV lines of these ions. In particular, scattering of anisotropic radiation in the forbidden magnetic-dipole coronal 7894, 10747, 5304 and 39277 Å lines followed by isotropic collisional excitation induces atomic polarization in numerous high-excited levels of the abovementioned ions. Spontaneous emission from these levels results in many permitted E1 EUV lines with a high degree of the fractional linear polarization. Among them we selected rather strong ones with high values of the Hanle critical magnetic field B_H which are Hanle-insensitive to the magnitude of the weak coronal magnetic field. However, the linear polarization in these selected lines can be explored to probe the orientation of the coronal magnetic field. We also found quite a large number of the EUV lines with relatively low B_H values. As a consequence, the linear polarization signal in the latter lines have to be affected by the Hanle effect in the weakly magnetized regions, so their linear polarization may be used for measuring the magnitude of the weak coronal magnetic field.

Small-Scale Activity and Magnetic Reconnection: an Overview of GST Results

Vasyl Yurchyshyn

Big Bear Solar Observatory, New Jersey Institute of Technology

High resolution solar telescopes allow us to peer deeply into rapidly varying chromosphere and the underlying photosphere. Here I will review recent findings related to small-scale activity in a quiet Sun based on data from Goode Solar Telescope.

Particle acceleration in 3D reconnecting current sheets with magnetic islands in solar flares and interplanetary environment

V. Zharkova

Northumbria University, Newcastle; ZVS research enterprise Ltd. London, UK

In this talk I will present the key issues associated with proton and electron acceleration in 3D reconnecting current sheets formed by interacting magnetic loops in solar flares, Heliospheric Current Sheet (HCS) and current sheets associated with interplanetary coronal mass ejections. These will include topology of acceleration of transit and bounced particle of the same charge, diMerent energy and pitch angle distribution of bounced and transit particles and their observational validation. We also will discuss separation of electrons and protons with respect to the current sheet midplane, formation of polarisation electric field across the current sheet and its role in defining proton and ion profiles in crossing the HCS and other current sheets. We present energy and pitch-angle distributions of accelerated particles in a single RCS (X-nullpoint) and in RCS with magnetic islands (X and O-nullpoints) and compare the simulations for different spacecraft crossing with the Parker mission observations. In conclusion we present 3D PIC simulations of reconnecting current sheet with formation of magnetic islands and evaluate timescale and nature of kinetic turbulence generated by accelerated electrons and protons, its distribution at various points of a current sheet. We also evaluate the frequency distribution of kinetic turbulence generated at different parts of reconnecting current sheet with magnetic islands.

RELATIVISTIC GRAVITATION AND COSMOLOGY

ASTRONOMY AND SPACE PHYSICS IN KYIV UNIVERSITY

Non universality of a_0 in MOND

A. Del Popolo

Catania University, Via Santa Sofia 78, 95123 Catania, Italy

The Lambda CDM model is correctly describing a large amount of observations, but it shows several issues as the Hubble parameter tension, the small scale problems, the cosmological constant problem, the non detection of dark matter, etc. Several modified theories of gravity try to reobtain the success of the LambdaCDM model without taking into account dark matter and dark energy, and assuming a theory of gravity different from that of Newton or general Relativity. One of those theories, the simplest, is MOND. This theory is based on the existence of a universal acceleration, a_0. In the case of accelerations, a, much larger than a_0, the gravitational theory reduces to Newton theory, while for a much smaller than a_0, Newton theory is modified. I show that a_0 is an emergent phenomenon depending from several physical quantities.

Separating the spectral counterparts in NGC 1275/Perseus cluster in X-rays

E. Fedorova[1,2], L. Zadorozhna[3,4,5], A. Tugay[3], N. Pulatova[5,6,7], A. Ganz[4,8], O. Gugnin[2]

[1]INAF - Osservatorio Astronomico di Roma, Rome, Italy;
[2]Astronomical Observatory Taras Shevchenko National University of Kyiv, Kyiv, Ukraine;
[3]Taras Shevchenko National University of Kyiv, Kyiv, Ukraine;
[4]Jagiellonian University, Faculty of Physics, Krakow, Poland;
[5]Niels Bohr Institute, Kobenhavn, Denmark;
[6]Main Astronomical Observatory of the National Academy of Sciences of Ukraine, Kyiv, Ukraine;
[7]Max-Planck-Institut fur Astronomie, Heidelberg, Germany;
[8]Leibniz University Hannover, Institute for Theoretical Physics, Hannover, Germany

We present the model-independent method for separating the spectral counterparts of the active galactic nucleus (AGN) NGC 1275 from the

surrounding emission of the Perseus cluster, as observed by Suzaku/XIS cameras. The Perseus cluster emission extends to higher energies than typically observed in AGN environments, reaching up to 9-10 keV. This necessitates precise separation of AGN and cluster spectra. To circumvent the degeneracy arising from numerous spectral fitting parameters, including elemental abundances, thermal and Compton emissions from the nucleus, and spectral parameters of the jet synchrotron self-Compton/inverse Compton emissions, we avoid traditional spectral fitting methods. Instead, we leverage spatial resolution and employ a double background subtraction approach. We apply this procedure to the complete set of Suzaku/XIS observational data for NGC 1275, resulting in cleaned spectra and a light curve of the AGN emission in this system. To demonstrate the applicability of our method, we also utilized the
available XMM-Newton/EPIC data.

The result of the monitoring of the selected isolated AGNs in the optical range for 2021 at the Terskol Observatory

Izviekova I.[1,2], Vavilova I.[1], Butenko G[2], Tarady V[2].

[1]Main Astronomical Observatory of NAS of Ukraine, Kyiv, Ukraine
[2] ICAMER Observatory of NAS of Ukraine, Kyiv, Ukraine

The results of spectro-photometric observations of the selected isolated galaxies with active nuclei conducted in July-August 2021 at the Terskol Observatory are presented. The Zeiss-600 and Zeiss-2000 telescopes were used. All objects are of the Seyfert type activity. The detailed photometry for most of them has not been carried out before. Among the main objects of observations: MCG+09-25-022, UGC10120, UGC10244, PGC86291, NGC6951, UGC12282, NGC7479, IC5287, and IC1495. The work presents the data processing of optical monitoring and research of short-term (STV) and intraday (IDV) variability of these specified objects.

ASTRONOMY AND SPACE PHYSICS IN KYIV UNIVERSITY

SPARC galaxies prefer Dark Matter over MOND

M. Khelashvili,[1,2,3,4] A. Rudakovskyi,[3] and S. Hossenfelder[4,5]

[1] Goethe Universität, Frankfurt am Main, Germany
[2] Department of Physics, Princeton University, Princeton, USA
[3] Bogolyubov Institute for Theoretical Physics of the NAS of Ukraine, Kyiv, Ukraine
[4] Frankfurt Institute for Advanced Studies, Frankfurt am Main, Germany
[5] Munich Center for Mathematical Philosophy, Munich, Germany

We currently have two different hypotheses to solve the missing mass problem: dark matter (DM) and modified Newtonian dynamics (MOND). In this work, we use Bayesian inference applied to the Spitzer Photometry and Accurate Rotation Curves (SPARC) galaxies' rotation curves to see which hypothesis fares better. For this, we represent DM by two widely used cusped and cored profiles, Navarro-Frenk-White (NFW) and Burkert. We parameterize MOND by a widely used radial-acceleration relation (RAR). Our results show a preference for the cored DM profile with high Bayes factors in a substantial fraction of galaxies. Overall, our analysis comes out in favor of dark matter.

Can Black Holes or Other Relativistic Space Objects be a Source of Dark Energy?

S.L. Parnovsky

Astronomical observatory of Taras Shevchenko National University of Kyiv, Kyiv, Ukraine

We consider the hypothesis that the sources of dark energy (DE) could be black holes (BHs) or more exotic objects, such as naked singularities or gravastars. We propose a definition of the presence of DE in the Universe and a criterion for what can be considered the source of this dark energy. It is based on the idea of the accelerated expansion of the Universe, which requires antigravity caused by large negative pressure. A recently proposed hypothesis, that the mass of BHs increases with time according to the same law as the volume of the part of the Universe containing it and the population of BHs can mimic DE, is examined. We demonstrate the reasons

why it cannot be accepted, even if all the assumptions on which this hypothesis is based are considered true.

The analysis shows that the source of DE cannot be ordinary black holes, naked singularities with positive mass and their combinations. Any object that attracts surrounding matter cannot be a DE source. This applies to any object surrounded by an accretion disk or one around which other bodies orbit. Naked singularities with negative mass provide antigravity but cannot mimic DE. Hypothetical gravastars have DE inside, and it is strange to consider them as a source of DE.

Quantum Entanglement and Superluminal Transmission of Information

S.L. Parnovsky

Astronomical observatory of Taras Shevchenko National University of Kyiv, Kyiv, Ukraine

The paradox about the supposedly instantaneous transfer of information associated with the determination of the parameters of one of the particles included in a quantum entangled pair is considered. It is shown that this conclusion is drawn on the basis of not quite correctly formulated conditions of the thought experiment underlying the imaginary paradox. A new parameter related to decreasing the correlation of states of particles which were initially entangled is proposed.

The quantum entanglement is a quantum mechanical phenomenon in which the quantum states of two or more objects are interdependent. For example, one can get a pair of photons in an entangled state, and then if, when measuring the spin of the first photon, its helicity turns out to be positive, then the helicity of the second should be negative, and vice versa.

The existence of quantum entanglement has been confirmed in numerous experiments and is not questioned. I want to discuss some aspects related to the paradox usually associated with this concept, limiting myself to a discussion of simple thought (gedanken) experiments.

The paradox associated with the existence of a pair of quantum entangled objects is connected with the fact that a measurement of a parameter of one particle is accompanied by an instantaneous termination of the entangled state of the other. In the simplest example, a pair of entangled photons is born somewhere in space. One of them arrives on Earth, where physicists measure its helicity. This makes it possible to know the helicity

of the second photon, which is somewhere in the Andromeda Nebula at that moment. Is this a transmission of information at faster than the speed of light in a vacuum forbidden by the special theory of relativity? I am going to show that the paradoxicality of this situation has much to do with its formulation.

The phenomenon of quantum entanglement has been confirmed by experiments. However, the analysis carried out showed that in reality paradox about the supposedly instantaneous transmission of information does not exist. The conclusion about the possibility of instantaneous transmission of information was made on the basis of not quite correctly formulated conditions of the gedanken experiment that underlay the imaginary paradox. An essential detail of the analysis is the well-known statement of quantum mechanics about the influence of the process of measurement, in this case, observation, on the state of the observed system.

Discreteness effects in cosmological simulations of warm dark matter

Yu. V. Shtanov[1,2] and V. I. Zhdanov[2]

[1]Bogolyubov Institute for Theoretical Physics, Kyiv, Ukraine
[2]Taras Shevchenko National University of Kyiv, Kyiv, Ukraine

In cosmological simulations, thermal velocities of warm dark matter particles are sometimes taken into account by adding random initial velocities to the simulation particles. However, a particle in the *N*-body system represents a huge collection of dark-matter particles, with average thermal velocity very close to zero. We provide a theoretical justification of the procedure of adding thermal velocities in *N*-body simulations and build a simple model of their influence on the power spectrum. Our model captures the physical effect of suppression of the power spectrum at small wave numbers and also explains its artificial enhancement at large wave numbers, observed in numerical simulations with added thermal velocities. The cause of this enhancement is the disturbance of the growth rate of the density profile introduced when adding random initial thermal velocities. The model predicts a turnover scale beyond which the simulated power spectrum is dominated by the discreteness effects, growing as $P(k) \sim k^2$, which is in a good agreement with numerical simulations.

Electrovac equations in the case of outgoing one-way null fields

Y.V. Taistra

[1]Pidstryhach Institute for Applied Problems of Mechanic and Mathematics NAS of Ukraine, Lviv, Ukraine

High-energy processes in astrophysics can generate strong electromagnetic fields, and their energy-momentum curves space-time, so Einstein-Maxwell equations are considered as model of propagation both electromagnetic and gravitational fields. When the Maxwell field has no sources, such a model is called electrovac. There are also additional assumptions on Maxwell field to investigate different simplest configurations of electromagnetic and gravitational fields. One of them is the well-known Kerr-Newman solution of the Einstein-Maxwell equations.

Considering equations in the spinor and Newman-Penrose tetrad calculus we can provide another assumption on electromagnetic field called one-way null field. These are fields propagating along gravitational field null directions. Gravitational field can be considered similarly. We present our results for electrovac in the case of one-way null fields.

Instability of spherically symmetric configurations in the quadratic f(R) gravity

V. I. Zhdanov[1], O. S. Stashko[2,3], Yu. V. Shtanov[1,4]

[1]Taras Shevchenko National University of Kyiv, Kyiv, Ukraine
[2]Department of Physics, Princeton University, Princeton, USA
[3]Goethe Universität, Frankfurt am Main, Germany
[4]Bogolyubov Institute for Theoretical Physics, Kyiv, Ukraine

We study stability of spherically symmetric configurations of the quadratic *f(R)* gravity. In case of a purely gravitational system, we have determined the global qualitative behavior of the metric and the scalaron field in the Einstein frame for all static solutions satisfying the conditions of asymptotic flatness. These solutions are proved to be regular everywhere except for a naked singularity at the center; they are uniquely determined by the total mass *M* and the "scalar charge" *Q* characterizing the strength of the scalaron field at spatial infinity. Approximation procedures are developed to derive asymptotic relations near the naked singularity and at spatial infinity, and

the leading terms of the solutions are presented. We investigate the linear stability of the static solutions with respect to the radial perturbations satisfying the null Dirichlet boundary condition at the center and numerically estimate the range of parameters corresponding to stable/unstable configurations. In particular, the configurations with sufficiently small Q turn out to be linearly unstable.

HIGH ENERGY ASTROPHYSICS

ASTRONOMY AND SPACE PHYSICS IN KYIV UNIVERSITY

Gamma-ray emission of the Shapley Supercluster

V.M. Babur[1], V.V. Voitsekhovskyi[2], B.I. Hnatyk[3]

[1]Taras Shevchenko National University of Kyiv, Kyiv, Ukraine
[2] University of Geneva, Geneva, Switzerland
[3]Astronomical Observatory of Taras Shevchenko National University of Kyiv, Kyiv, Ukraine

This research aims to model and investigate the gamma-ray spectrum of the Shapley Supercluster, one of the largest and most massive structures in the nearby Universe, located approximately 200 Mpc away. Utilizing the MINOT software (Modeling the Intracluster Medium (Non-)Thermal Content and Observable Prediction Tools), we develop the theoretical framework underlying the gamma-ray emission, with a particular focus on hadronic interactions of accelerated cosmic ray nuclei with the nuclei of the intracluster medium. Our modeling is based on observational data from the recent eROSITA-DE Data Release 1 (DR1). The results obtained from our simulations are used to analyze the feasibility of detecting very high energy gamma-ray emission from the central region of the Shapley Supercluster using the Cherenkov Telescope Array Observatory (CTAO), a next-generation ground-based gamma-ray observatory. This study not only aids in guiding future observational strategies but also enriches our understanding of cosmic ray distribution and interaction mechanisms in large-scale structures.

Search for sources of EHECR: simulation-based backpropagation of cosmic rays near the Local Void

O. Gugnin[1], V. Voitsekhovskyi[2], B. Hnatyk[3]

[1] Taras Shevchenko National University of Kyiv, Kyiv, Ukraine
[2]University of Geneva, Geneva, Switzerland
[3]Astronomical Observatory of Taras Shevchenko National University of Kyiv, Kyiv, Ukraine

Determining the origins of extremely high-energy cosmic rays (EHECRs) is a crucial goal in high-energy astrophysics, given that their extreme energies challenge existing particle acceleration mechanisms. Clarifying the sources and propagation characteristics of EHECRs with various compositions will

illuminate the most violent and energetic processes in the Universe, possibly involving environments surrounding magnetars or other exotic astrophysical phenomena. In the current study, we utilized numerical simulations to examine the propagation of EHECRs with different chemical compositions (protons, helium nuclei, carbon nuclei, and iron nuclei) in the vicinity of the local void using the CRPropa library. Our analysis involved tracking the three-dimensional trajectories of these EHECRs within the Milky Way galaxy. To assess the connection between the EHECRs and objects in the local void as potential sources, we conducted a statistical analysis and visualized two-dimensional projections of the particle trajectories to identify other possible source candidates along the EHECRs' paths.

Numerical simulations of early supernova remnants' evolution

T. Kuzyo[1], O. Petruk[1,2]

[1]Institute for Applied Problems in Mechanics and Mathematics NAS of Ukraine, Lviv, Ukraine
[2]Palermo Astronomical Observatory INAF, Palermo, Italy

Supernova remnants are essential sources of information about supernova progenitor star and conditions in the circumstellar environment where the supernova explosion occurs. The study of the transition features from a supernova to the supernova remnant is an important link for establishing a relationship between them.

Using full MHD simulations, we explore the magnetic field structure inside young supernova remnants, which is an important factor in the acceleration of cosmic rays and features of its non-thermal emission. Simulation results provide important information about the dynamics of the supernova remnant's shock wave and distribution of energy components in different supernova remnant parts. Also, we provide an analysis of the applicability limits of spherically-symmetric numerical solutions for supernova remnants evolution compared to a 3D case.

ASTRONOMY AND SPACE PHYSICS IN KYIV UNIVERSITY

Gamma-ray emission from the outskirts of magnetar SGR1900+14

V. Nikitchenko[1], V. Voitsekhovskyi[2], A. Sokareva [1]

[1]Taras Shevchenko National University of Kyiv, Kyiv, Ukraine
[2]University of Geneva, Geneva, Switzerland

The main goal of this study is to model the observed high-energy (HE, $\varepsilon >$ 100 MeV) and very high-energy (VHE, $\varepsilon >$ 100 GeV) γ-ray emission from the region of the magnetar SGR1900+14, located at a distance of 12.5 kpc. This non-thermal emission may be a promising manifestation/consequence of cosmic ray (CR) acceleration mechanisms. We investigate potential sources and processes capable of generating CRs with energies sufficient to produce the observed γ-ray emission. Among the options considered are a supernova remnant (SNR) and a pulsar wind nebula (PWN). Within these models, we made simulations implementing hadronic and leptonic scenarios to form the observed γ-ray emission. Since we associate the observed gamma-ray flux with the distant SGR1900+14, the parameters of observed radiation from Fermi-LAT, H.E.S.S., and HAWC telescopes require sources with large energy reserves of the order of 10^{52} erg. Such energies could be released during a Hypernova outburst, leading to the formation of the magnetar SGR1900+14.

We also show that recently discovered Supernova Remnants G043.023+0.762 and G043.070+0.558, at the distances of 3.8 kpc and 2.7 kpc respectively, could also be potential sources of this observed emission. The advantage of these sources are relatively close distances, that allow typical SNR energies.

Effect of the non-uniform velocity behind the strong shock on the radio spectrum of supernova remnants

O. Petruk[1,2], T. Kuzyo[1]

[1]Institute for Applied Problems in Mechanics and Mathematics NAS of Ukraine, Lviv, Ukraine
Palermo Astronomical Observatory INAF, Palermo, Italy

We generalize the approach of Bell to shock particle acceleration to the cases of nonuniform distributions of the flow velocity and apply it to acceleration of cosmic rays in supernova remnants. Accelerating particles

penetrate to different distances from the shock and are scattered off the centers with different speeds. Diffusion length depends on the particle momentum. Therefore, in general, the spectrum of accelerated cosmic rays might reflect diffusion properties and spatial structure of the flow. This effect is known to be important in case of the non-linear acceleration when particles themselves modify the flow upstream of the shock. We analyze the cases where the flow velocity behind the supernova remnant shock is not uniform, as result of the hydrodynamic evolution. It appears that the cosmic rays with maximum momenta may probe the flow structure up to 10% of SNR radius. This could lead to a sort of a convex shape of the spectrum, contrary to the non-linear regime which results in the concave shape. We discuss possible influence of the non-uniformity of plasma velocity on the radio indices of supernova remnants.

Ultrarelativistic gravity and extremely energetic cosmic ray

R.M. Plyatsko, M.T. Fenyk

[1]Pidstryhach Institute for Applied Problems in Mechanics and Mathematics, Lviv, Ukraine

In 1959, Pirani attracted attention to properties of the ultrarelativistic gravity according to general relativity. He showed that the gravitational field of a fast-moving Schwartzschild's mass bears an increasing resemblance to a gravitational plane-wave field, the greater the speed of the mass. It follows from this paper that the amlitude of the wave is proportional to the second power of the relativistic Lorentz factor. Later the encounters between black holes were considered in the limit that the approach velocity tends to the speed of light. In 1990th, Mashhoon critically examined the notion of gravitational field strength and showed that this concept is strongly observer dependent, and impulsive tidal acceleration of a beam of ultrarelativistic particles were studied in the gravitational field. In the recent paper Fokas A.S. Eur.Phys.J.C. 2019,**79**, 271 it is stressed that the ultrarelativistic gravitational force acting on the two particles has properties usually associated with the strong force, and in Feng J.C. arXiv:2401.05764 it is summarized that various authors have pointed out that gravitational effects can be greatly amplified in the frame of an observer moving close to the speed of light.

The two types of the tidal acceleration are considered: the first is caused by the gravitoelectric components which act on a beam of particles moving

in Schwartzchild's field, and the second is caused by the gravitomagnetic components in Kerr's field. It was shown that in the rest frame of the fast-moving composite system, the tidal accelerations could be proportional to the second power of the relativistic Lorentz factor.

The next stage of investigation of the ultrarelativistic gravity is connected to the consideration of the properties of the spinning test particle motions in Schwartzchild's field. It was shown in Plyatsko R. Phys. Rev. D. 1998, V. **58**, 084031 that in this field the spin-gravity acceleration in the rest frame of the spinning particle is caused by the gravitomagnetic components. In the ultrarelativistic limit, the value of this acceleration is proportional to the second power of the relativistic Lorentz factor. Now we discuss possible role of this acceleration in the context with the results of paper Abbasi R.U. et. al. Science, 2023, V. **382**, 903 for the extremely energetic cosmic ray.

High energy astrophysical neutrinos from the main clusters of the Shapley Supercluster

M. Poleshchuk[1], V. Babur[2], L. Zadorozhna[2,3]

[1]Bogolyubov Institute for Theoretical Physics NAS of Ukraine, Kyiv, Ukraine
[2]Taras Shevchenko National University of Kyiv, Kyiv, Ukraine
[3]Niels Bohr Institute, Copenhagen, Denmark

Modern multi-messenger astronomy relies on integrating diverse observations from multiple instruments and messengers to unravel the mysteries of the universe. Neutrinos, due to their low scattering cross-section compared to photons and other particles, offer a unique avenue for studying astrophysical phenomena. When combined with gamma-ray observations, they provide valuable insights into cosmic processes. The Shapley Supercluster, the one of the largest known galaxy super clusters, serves as an excellent target for observational studies, shedding light on galaxy evolution and cluster-scale mass assembly. This study will focus on all the main clusters within the Shapley Supercluster, providing a comprehensive analysis of this massive structure.

Additionally, we will investigate the Perseus Cluster as a baseline galaxy cluster model for observations with the CTAO gamma-ray observatory and the IceCube neutrino observatory. By leveraging ultrahigh energy neutrino observations, we aim to enhance our understanding of these astrophysical phenomena. By harnessing the capabilities of neutrino observatories, we

intend to deepen our knowledge of the fundamental workings of the universe, using the Shapley Supercluster and the Perseus Cluster as key observational targets.

Exploring dark matter signatures in gamma-ray observations: a study of the Shapley Supercluster and the Perseus Cluster

M. Stepanov[1], L. Zadorozhna[1, 2], V. Babur[1]

[1]Taras Shevchenko National University of Kyiv, Kyiv, Ukraine
[2]Niels Bohr Institute, Copenhagen, Denmark

The existence of dark matter (DM) has been inferred from various astronomical observations, suggesting it as a crucial component of the universe. Despite its prevalence, the properties of DM remain largely unknown, with only gravitational interactions observed thus far. Proposed extensions of the Standard Model (SM) suggest various candidates for DM particles, spanning a wide mass range. The DM particle could manifest itself through SM particles, decaying or annihilating to photons. For instance, the identification of gamma-rays resulting from interactions of massive DM candidates, such as WIMPs – Weakly Interacting Massive Particles, has rapidly become a highly promising avenue. WIMPs, with masses typically in the GeV range, are a natural consequence of several extensions of the SM aimed at resolving the gauge hierarchy problem and explaining the mechanism behind electroweak symmetry breaking.

In this investigation, we conduct a comprehensive analysis of the gamma-ray emission resulting from DM annihilation and decay within a smooth DM distribution, excluding the influence of substructures and clumps. Using the publicly available CLUMPY code, we compute the gamma-ray fluxes originating from DM in the four central clusters of the Shapley Supercluster and compare them with those from the Perseus Cluster. This involves calculating astrophysical J- and D-factors using the DM-density profile along the line of sight for DM annihilation/decay. The signal stemming from the decay of DM particles correlates directly with the total mass of DM within the concerning object, whereas the signal from annihilation is proportional to the square of the DM density. Hence, the decay of DM particles results in a notable increase in the signal, particularly for more massive objects. We also evaluate the potential for future detection of gamma-ray fluxes from DM within clusters using estimated sensitivity curves for upcoming next-generation instruments like CTAO.

Dynamic processes in jets of active galactic nuclei according to radio astronomical observations

D.A. Zabora, M.I. Ryabov, A.L. Sukharev

[1]Odesa observatory URAN-4, Institute of Radio Astronomy NAS of Ukraine, Odesa, Ukraine

MOJAVE is one of the most effective VLBI monitoring programs to observe Active Galactic Nuclei (AGN) jets angular structure in the radio band. MOJAVE are using the radio interferometric network of 10 radio telescopes of the National Radio Astronomy Observatory (NRAO, USA). Observation results are available in the MOJAVE Database (MOJAVE/2cm Survey Data Archive). With the largest database of about 8600 km, the system allows to map AGN's close surroundings at ~0.12 mas resolution on ~15.4 GHz frequency. For approximately 30 years of MOJAVE AGN monitoring observations, the Survey Data Archive accumulated a huge amount of observation data. Especially interesting ones are data about the locations of bright features (components) in jets and their changes in time. This data is presented in image format (Separation vs. time plot). And their presence allows to analyze motion patterns of components in jets, which represent AGN's activity, as well as the jet's structure itself. In this work analysis of components motion in the Seyfert I galaxy 3C 120 (1995.6 – 2020 yy, 54 components), quasars 3C 273 (1995.6 – 2020 yy, 31 components) and 3C 454.3 (1995.4 – 2019 yy, 9 components), BL Lac (1995.3 – 2020 yy, 37 components) was performed. These objects demonstrate presence both of moving and quasistationary components, which slowly change their locations in time. Based on the moving components, the average velocities and accelerations in the jets were estimated in projection onto the picture plane. Also, the distribution of velocities of the components in the jets was constructed and assumptions were made about the structure of the jets based on existing publications on them. The discussed components demonstrate inhomogeneities in their movement up to quasi-harmonic oscillations of their positions relative to the average movement direction trend. Especially interesting are the oscillations of quasi-stationary components close to nuclei, which can be a result of the propagation of shock waves in jets.

ASTROMETRY AND SMALL BODIES OF THE SOLAR SYSTEM

Comet 67P/Churyumov-Gerasimenko in the 2021/2022 apparition: Preliminary results of observations

V. Rosenbush[1,2], O. Ivanova[1,2,3], I. Luk'yanyk[1], V. Kleshchonok[1,4], O. Shablovinskaya[5]

[1] Astronomical Observatory of Taras Shevchenko National University of Kyiv
[2] Main Astronomical Observatory of National Academy of Sciences of Ukraine, Kyiv, Ukraine
[3]Astronomical Institute of Slovak Academy of Sciences, Tatranska Lomnica, Slovak Republic
[4] Max Planck Institute for Solar System Research, Göttingen, Germany
[5] Núcleo de Astronomá de la Facultad de Ingenierá, Universidad Diego Portales, Santiago, Chile

Comet 67P/Churyumov-Gerasimenko (67P/C-G) is a well-studied comet of the Jupiter family. During the previous apparition, we extensively studied it in the post-perihelion period using the 6-m BTA telescope (Rosenbush et al. 2017; Ivanova et al. 2017). Now, in the recent 2021/22 apparition, we aimed to compare our findings with those of 2015/16. We conducted comprehensive pre- and post-perihelion observations with various telescopes, providing important insight into the composition and evolution of the comet.

Quasi-simultaneous photometric, spectroscopic, and polarimetric observations of comet 67P/C-G were conducted at the 6-m BTA telescope (SAO) on October 6, 2021 with the g- and r-sdss filters and on February 6, 2022 with continuum BC (λ4450/62 Å) and RC (λ6839/96 Å) and emission CN (λ3870/58 Å) filters. In addition, aperture polarimetry of the comet was carried out at the 2.6-m of the CrAO and 2-m telescopes of the Peak Terskol Observatory. These observations cover a range of heliocentric distances from 1.248 au to 1.836 au, geocentric distances from 0.468 au to 0.950 au, and phase angles from 10.5° to 48.2°.

Comet 67P/C-G was active and showed an extensive coma with jets and a dust tail. On October 6, 2021, –31 days before passing perihelion, the sunward jet and long dust tail are detected in the images of the comet. The structure of the dust coma of the comet changed significantly during post-perihelion observations on February 6, 2022 (+96 days after perihelion) in comparison with pre-perihelion images. The enhanced images showed two jets which are located symmetrically relative to the rotation axis of the

nucleus. However, the most prominent feature of these images is a bright linear strip-like structure extending in the direction of the Sun, which is similar to the neck-line structure. Using a geometric model, we found that two observed jets are formed from the same active area located at a latitude of $\varphi = -58° \pm 5°$ and the opening angle of the jet is $26° \pm 8°$. We also studied the unusual morphology of the CN coma in the comet and showed how it can be formed.

Strong CN and relatively weak C_2, C_3, and NH_2 emissions are identified in the spectra of the comet in 2021 and 2022. The production rates of CN, C_3, and C_2 are in good agreement with data obtained by other authors. The production rate ratio $\log[Q(C_2)/Q(CN)]$ is -0.2 ± 0.4 for 2021, and -0.6 ± 0.1 for 2022, respectively, which corresponds to the carbon-chain depleted class of comets. However, this conclusion has to be taken with caution, because, as Le Roy et al. (2015) showed, comet 67P/C-G can be carbon-chain depleted in the summer hemisphere, whereas for the winter hemisphere, the comet would be carbon-chain normal. The dust production rate $Af\rho$ is smaller than 200 cm for both periods of observations.

The dust color (g–r) gradually changed from 0.8 mag within the innermost coma to about 0.2 mag in the outer coma and the spectral slope was 13.6 ± 0.3 percent/100 nm for observations in 2021. In October 2021, the polarization in the near-nucleus area was about 11% at a phase angle of 47.9° and practically did not change over the coma. In February 2022, at a phase angle of 10.5°, the polarization varied between –1% in the near-nucleus area and –2.5% in the outer coma. In general, the polarization phase curve of comet 67P/C-G resembles that of a highly polarized dust comet, however, it seems that higher polarization values are observed specifically in the 2021/22 apparition. Using our photometric and polarimetric observations of the comet, we intend to model the physical characteristics of the dust environment in the comet.

References

Ivanova O.V. et.al. 2017. MNRAS 469, Issue 2. 386-395.
Le Roy L. et al. 2015. A&A 583, A1
Rosenbush V.K. et al. 2017. MNRAS 469, 475-491.

Detection of manifestations of the non-gravitational effects in the movement of comet Encke using materials of the Astronomical Museum

A. Kazantsev, L. Kazantseva

Astronomical observatory of Taras Shevchenko National University of Kyiv

Among the materials of the Astronomical museum of the Astronomical observatory there are many interesting documents about the observations of separate small bodies in the past years. One of them is a map with a star field, on which the position of a comet is indicated in 1821. The text of the signature is not entirely clear, it is written in Latin letters using English, Latin and even Greek terminology. It is noted that it shows the positions of the comet (Cometa Enckani) from July 24 to September 15 in the constellation Pisces. Previous calculations showed that it may be comet Encke. At the same time, the calculated positions differed from the given ones by approximately 4^{o}, which indicates on an action of the non-gravitational effects (NGE).

Differences between the observed positions of comet Encke and the calculated ones (O – C) taking into account only the gravitational influence of the bodies of the Solar System from 2020 to 1821 were found. At that, archival data of the International Minor Planet Center (MPC) were used, where the oldest observations of comet Encke date back to 1852. The most clear manifestations of the NGE in the comet's motion are significant differences in the O – C values at the different heliocentric distances of the comet during a single rotation around the Sun. The course of the O – C dependence over time may indicate a gradual decrease of the NGE from the 19th century to the present time. However, such a dependence may be influenced by the choice of the epoch of the initial elements of the comet's orbit, which are used in the calculations.

Analysis of the text on the 1821 map and calculations shows that these observations were not made in Russia. It is most likely that these are the observations of Heinrich Olbers, which got in Kyiv observatory when a part of his library was transferred from the Pulkovo Observatory in 1842.

Short-term dust color variations of distant comets

A. Voitko[1], O. Ivanova[1,2]

[1]Astronomical Institute of the Slovak Academy of Sciences, Tatranska Lomnica, Slovak Republic
[2]Main Astronomical Observatory of National Academy of Sciences of Ukraine, Kyiv, Ukraine

Comets are small bodies of the Solar system that differ by their activity. Release or sublimation of volatiles can drag dust particles out of the nucleus. As a result, gas and dust particles form a coma around the nucleus. However, at large heliocentric distances, the radiation registered from a comet contains primarily solar light scattered by dust particles, while contamination of gaseous emissions can be negligible. One of the basic photometric characteristics of a dust cometary coma is color, which reflects the effectivity of light scattering by dust particles at different wavelengths. It depends mainly on the size distribution and chemical composition of grains. Reports about dust color variation first appeared at the end of the previous century. Nevertheless, this phenomenon remained poorly studied.
We started to collect monitoring observations of comets to search for dust color variations, which occurred during a few days or weeks. Mainly, we use archive data obtained at the Skalnaté Pleso Observatory and recently taken observations. We selected comets observed at heliocentric distances larger than 3 au. As a result, we got data for 5 long-period and 5 hyperbolic comets. Additionally, we have analyzed dust color variations in the coma of short-period comet 29P/Schwassmann-Wachmann 1 in observations of two outbursts in October 2018 and November 2020. Concerning the other comets, dust color variations were mainly found for long-period comets. However, it can be caused by a relatively small amount of the sampled objects. So, we supplement our data with the results from the literature to get more information about the frequency of occurrence and possible causes of dust color changes.

Data analysis for asteroid binaries and pairs as a test of their formation model

A. Aleksandrov[1], O. Golubov[1,2]

[1]School of Physics, V. N. Karazin Kharkiv National University, Kharkiv, Ukraine,
[2]Institute of Astronomy, V. N. Karazin Kharkiv National University, Kharkiv, Ukraine

The report presents the results of the study of the evolution of binary asteroid systems and asteroid pairs in the inner part of the main asteroid belt. Based on the statistical analysis of the data, the typical sizes of satellites in binary asteroid systems are determined and the lifetimes of single and binary asteroids of different sizes under the influence of the YORP effect are calculated. The model is analyzed, which assumes that single asteroids form binary systems by reaching the critical rotation speed due to the YORP effect, and then decay into asteroid pairs as the BYORP effect increases the radii of their orbits. We find that asteroids spend about 7% of their time in the binary state, which is consistent by the order of magnitude with the observed fraction of binary asteroids of 15%.

The distribution of young asteroid pairs by age is investigated and the frequency of their formation is estimated, taking into account the incompleteness of the sample of known asteroids. Theoretical estimates of the fraction of binary asteroids in three size groups are obtained: 2% for diameters of 1-3 km, 13% for 3-5 km, and 6% for 5-10 km, which is again consistent by the order of magnitude with the expected 15%. These results show that the rotational decay of asteroids and the subsequent BYORP disintegration of binaries as key mechanisms for the formation of asteroid pairs, which are no less significant than collisions. The hypothetical states of the YORP equilibrium of single and binary asteroids do not play the dominant role in their dynamical evolution.

First results of broadband observations of selected comets with SkyMapper telescope

S. Borysenko[1], A. Baransky[2], O. Sokoliuk[1]

[1]Main Astronomical Observatory of NASU, Kyiv, Ukraine
[2]Astronomical Observatory of Taras Shevchenko Kyiv University, Kyiv, Ukraine

Broadband observations of selected comets were started at the Siding Spring observatory (Q55) in January 2024 by International Ukraine – Australian Grant support. Most interesting active objects – quasi-Hilda comets, active asteroids, quasi-Trojan comets, some trans-Jupiter comets (centaurs), and some dynamically new and distantly active non-periodic comets with magnitudes up to 20^m were selected for researches.

180 observational hours (20 observational nights) were obtained by International Ukraine – Australian Grant support for broadband observations with a 1.35-m telescope SkyMapper at Siding Spring observatory. The telescope's advanced 1.35-m modified Cassegrain optics has an f4.79 focal ratio, making the system highly efficient as a survey instrument. At the heart of the telescope is a unique digital camera designed and constructed in-house by ANU technicians. The A$2.5 million camera uses 268 million pixels (0.496″/pix) to capture a region of sky 32 × 34′ × 17′. SkyMapper telescope has fully automated system for operating, focusing and shooting of images and equipped with broadband SDSS system of filters (*griz*). SkyMapper has additional, distinctive ultraviolet filters, a Strömgren system-like *u*, and a unique narrow *v* near 4000Å.

The wide field of CCDs also allows to register the dozens of asteroids. Some part of the registered objects was measured by *Astrometrica* software and MPC reports were published. The resulting images of comets will also be measured to obtain their physical characteristics and modeling of the dust atmospheres of the comets.

ASTRONOMY AND SPACE PHYSICS IN KYIV UNIVERSITY

Simulation of the meteor light curve taking into account the chemical composition of the meteoroid determined from spectral observations

O. Golubaev[1], A. Mozgova[2]

[1]Institute of Astronomy of V. N. Karazin Kharkiv National University, Kharkiv, Ukraine
[2]Astronomical Observatory of Taras Shevchenko National University of Kyiv, Kyiv, Ukraine

We present a method of model reproduction of the light curves of selected meteors taking into account the physical and chemical parameters of meteoroids obtained from spectral observations. Such an integrated approach with the use of spectral data makes it possible to assess the physical parameters of meteoroids more unambiguously, in contrast to the classical method. The classical method of estimating the mass, average density and porosity of a meteor body is derived from the equations of deceleration, mass loss (ablation) and luminosity of a meteor. In this case, the simulation relies only on the energy balance equation, where there is no information about the chemical composition of meteoroids and an accurate interpretation of the interaction of particles with the atmosphere in terms of the kinetic properties of meteoroids.

The meteor data analyzed in this work were obtained from observations using the Automated Video Spectral Meteor Patrol (AVSMP) of the Institute of Astronomy of V. N. Karazin Kharkiv National University. We present the results of research of selected meteors brighter than 0^m that were recorded by the multi-stations method and for which spectral observations were obtained.

Aerosols of cosmic origin in earth atmosphere: the meteor showers influence

P. Kozak

Taras Shevchenko National University of Kyiv, Astronomical Observatory, Kyiv, Ukraine

The interaction of cosmic particles belonging to some meteor streams with earth atmosphere is considered. The input parameters of the meteor shower meteors are their mass, velocity, and the radiant zenith angle (the angle of entrance of space particles into atmosphere). Since the velocity is constant

value for the given meteor stream, only two parameters are considered as variants. The radiant zenith angles depend on time because of the position of the earth inside the meteor stream. Taking into account the earth rotation it was determined that the meteor influx depends on the latitude and longitude for some atmosphere square (conditionally we can call it as the position of the observer). Finally, the meteor mass is the main parameter, which forms the start formation profiles of aerosols from the meteor streams. The influence of the meteor streams onto aerosol profiles formation in upper atmosphere seriously differs from sporadic meteors contribution into this process. All formulae for calculation of the aerosol influx from any meteor stream are presented. The change of aerosols concentration along the altitude as a function of time is presented. The Perseid meteor stream was used as an example.

Acknowledgements: the work is done in the frame of financial support from the Ministry of Education and Science of Ukraine, the project number is No 22BF023-02.

Theory of the Yarkovsky force for asteroids with different shapes and thermal properties

O. Golubov[1], O. Mikhalchenko[1], V. Lipatova[2]

[1]Institute of Astronomy, V. N. Karazin Kharkiv National University, Kharkiv, Ukraine
[2]Institut für Theoretische Astrophysik, Zentrum für Astronomie, Heidelberg University, Heidelberg, Germany

The Yarkovsky effect is a recoil light-pressure force that originates due to the asymmetric emission of thermal infrared radiation by rotating asteroids. It has been confirmed observationally for about 300 asteroids. It manifests itself in the asteroid evolution via spreading out asteroid families into the Yarkovsky V-shapes, transporting the main-belt asteroids to resonances and thus helping to resupply the near-Earth asteroid population with new members. The practical significance of the Yarkovsky effect includes its application to determining asteroid densities and its crucial role in predicting asteroid collisions with the Earth. Despite the importance of the Yarkovsky effect, it is commonly analyzed either in an oversimplified linearized thermal model for a spherical asteroid or by complicated fully numeric simulation of individual asteroids.

In the talk, we will present an analytic theory for the Yarkovsky force, which is sufficiently precise to describe the available observational data but still sufficiently simple to see all the relevant parametric dependencies. We single out the dependence of the Yarkovsky force on the asteroid's thermal properties, shape, obliquity, and orbit.

For the thermal dependence, we compare the standard linearized thermal model (valid only for big thermal parameters) with the newly created perturbation theory (valid for small thermal parameters), combine their results in one smooth expression, and then improve its accuracy by fitting the free parameters of the expression to the results of the numeric simulation. We find out that the traditional linearized thermal model is tens percent wrong for thermal parameters of the order or smaller than unity, to which range the parameters of most studied asteroids belong.

Then we integrate the Yarkovsky force over the surface of spherical asteroids, ellipsoidal asteroids, and asteroids described by polyhedra. We find out that 3-axial ellipsoids give a good approximation to the Yarkovsky force, while spheres do not.

The results are combined into a new expression for the Yarkovsky effect. The revision of the orbital and obliquity dependence is still a work in progress.

Trojan asteroids on the Earth`s orbit and computer modeling of their motion

O. Polinko, Y. Lyashenko

Cherkasy Physics and Mathematics Lyceum, Cherkasy, Ukraine

There are small bodies orbiting around the L_4 or L_5 Lagrangian points of a Sun-planet system that are known as trojan asteroids. There is an assumption that the Earth's trojan asteroids came to us from the main asteroid belt between Mars and Jupiter. Using model calculations, here we present the results of our research, where we show that an asteroid from the main asteroid belt, due to the gravitational interaction with the Earth, can make such deviations from an elliptical orbit, after which the body will begin to move around the Lagrangian triangular points on the Earth`s orbit for a long time.

There were modeled twelve possible scenarios of the transition of a main-belt asteroid to the Earth's orbit in the region of triangular libration points. To make simulations we used a model that takes into account the N-

body gravitational attraction of the Sun and eight planets of the Solar System. We selected the Keplerian orbital elements of the main-belt body so that it would meet the Earth at a specific moment in time, they would gravitationally interact and the asteroid would change its orbit and begin to move around the L_4 or L_5 point on the Earth's orbit.

We also noticed similarities in the orbits of the already known Earth Trojan asteroid 2020 XL_5 and our simulated body. Such similarity in orbits tells us the possible orbital elements of the 2020 XL_5 that it acquired before it began to move around the L_4 libration point on the Earth's orbit.

To sum up, the simulation results show that an asteroid from the main asteroid belt can enter the Earth's orbit and achieve the status of a temporary Earth Trojan asteroid.

Centaur 174P/Echeclus: surface color from the post perihelion follow up observations

I.Kulyk[1], I. Luk'yanyk[2], O. Ivanova[1,3]

[1]Main Astronomical Observatory of the National Academy of Sciences of Ukraine, Kyiv, Ukraine
[2] Astronomical Observatory of Taras Shevchenko National University of Kyiv, Kyiv, Ukraine
[3] Astronomical Institute, Slovak Academy of Sciences, Slovak Republic

Centaur 174P/Echeclus have exhibited sporadic activity over the wide range of heliocentric distances. Since the discovery, Echeclus has covered approximately three-quarters of its orbit, passing perihelion in April 2015 [1]. During this period, the object has undergone four outbursts. In the 2005 there was the largest one ever detected for Centaurs meanwhile no emission lines were observed in the optical spectral range [2]. The unusual blue dust coma was revealed during the outburst happened in 2016. The amplitude of Echeclus' light curve varies along the orbit pointing out that a rotation axis is probably strongly inclined from the normal of its orbital plane [3,4].

Now Echeclus moves on its post perihelion orbit, which has not been covered by observations yet. We present the preliminary results of the photometric monitoring observations of 174P. The post perihelion Echeclus' images were obtained with the 2-m Liverpool Telescope during 6 sequential nights in October 2019. Since there are no signs of physical activity of the target, we use the B, V, R, I images to calculate the normalized reflectivity gradients in the BV, VR, RI spectral intervals (the surface color) and amplitudes of Echeclus' light curves in the different

spectral bands. Our results suggests, that the surface color varies with rotation phase pointing out the surface inhomogeneity, likely, as a result of the recent activity of 174P. More observations should be used to check this tentative conclusion.

References

[1] Marsden, B.G., *MPEC 2000-E64*, 2000. https://www.minorplanetcenter.net/mpec/K00/K0064.html.

[2] Choi, Young-Jun, Weissman, P., Discovery of Cometary Activity for Centaur 174P/Echeclus (60558), *Bulletin of the American Astronomical Society*, vol. 38, p.551, 2006. https://ui.adsabs.harvard.edu/abs/2006DPS....38.3705C.

[3] Kareta, Th.,Sharkey, B., Noonan, J., et al., Physical Characterization of the 2017 December Outburst of the Centaur 174P/Echeclus, *The Astronomical Journal*, vol. 158, Iss. 6, article id. 255, 10 pp., 2019. doi: 10.3847/1538-3881/ab505f.

[4] Rousselot, P., Kryszczyńska, A., Bartczak, P., et al., New constraints on the physical properties and dynamical history of Centaur 174P/Echeclus, *Monthly Notices of the Royal Astronomical Society*, vol. 507, Is. 3, pp. 3444-3460, 2021. doi:10.1093/mnras/stab2379.

Modernization of the AZT-8 telescope

I. Luk'yanyk[1], V. Karbovsky[2], M. Buromsky[1], V. Kleshchonok[1], M. Lashko[2]

[1]Astronomical Observatory of Taras Shevchenko Kyiv University, Kyiv, Ukraine
[2]Main Astronomical Observatory of NASU, Kyiv, Ukraine

The report is devoted to plans for the modernization of the AZT-8 telescope of the observed station of Taras Shevchenko National University of Kyiv in the village Lisnyky. The purpose of the modernization is to bring the technical condition of the telescope up to the modern technical level. Operational accessibility, automation of the observation process, quality of the received observational material, remote control via the Internet, quick verification of new ideas, provision of an innovative educational process in conditions of an epidemic or martial law were chosen as the key principles of modernization efficiency. The basis is the idea of a two-level architecture of the tool control system with a star connection topology, which allows for

the separation of control, control and executive systems, which, in turn, ensures the fulfillment of all the principles of modernization efficiency.

Optimization of video cameras positions and their optical characteristics for the special atmosphere and air space monitoring tasks

P. Kozak, I. Luk'yanyk

Taras Shevchenko National University of Kyiv, Astronomical Observatory, Kyiv, Ukraine

Modern investigation of the upper atmosphere, its middle part, some local air zones with the aim for non-interruptive monitoring of them is a very technically oriented problem. From one hand, the monitoring must be continues and with possibility to accumulate the maximal data base of all objects presented in the fields of view. For these purposes the video cameras with large fields of view must be used. On the other hand, the information about the known observable objects, or unrecognized objects must be obtained in the maximal volume, which needs to use the more long focus lenses and the cameras with higher temporal resolution which are much more expensive. Additionally, in some cases we need to use for précising the near infrared, thermal infrared (7-14 mkm) wave length bands, and even the spectral observations. But this investigation is limited by the selection of video cameras types for installing them into the ideally optimized positions in order to completely control the fixed air space with further transport of the observational data from the cameras to the server for the future processing in real time. The results of these investigations may be used for both astronomical and geophysical tasks, and for military purposes.
Acknowledgements: the work is done in the frame of financial support from the Ministry of Education and Science of Ukraine, the project "Mathematical sciences and natural sciences".

Lisnyky observational station contributions to GRANDMA collaboration

O. Pyshna[1], A. Baransky[1], A. Simon[2], V. Vasylenko[2], Y. Romaniuk[3], O. Sokoliuk[3]

[1]The Astronomical Observatory of Taras Shevchenko National University of Kyiv, Kyiv, Ukraine
[2]Astronomy and Space Physics Department, Taras Shevchenko National University of Kyiv, Kyiv, Ukraine
[3] Main Astronomical Observatory of NAS of Ukraine, Kyiv, Ukraine

GRANDMA (Global Rapid Advanced Network Devoted to the Multi-messenger Addicts) comprises worldwide telescopes of varied sizes, equipped with both photometric and spectroscopic facilities. The primary objective of the network is to monitor well-localized gravitational wave alerts, potential gravitational wave source candidates, bright afterglows of gamma-ray bursts, kilonova candidates, supernovae, and optical counterparts of neutrino sources. Lisnyky Observatory has been actively involved in collaboration activities since 2019, utilizing its Lisnyky-AZT8 and Lisnyky-Schmidt-Cassegrain telescopes to observe sources, achieving typical photometric upper limits of 20.5 and 18.5 in Rc, respectively. In this report, we provide a comprehensive summary of Lisnyky Observatory's contributions to the GRANDMA collaboration and the resulting scientific outcomes.

Lisnyky made data contributions by observing several objects, including the GW electromagnetic source candidate AT2019wxt, ZTF21abxkven and ZTF21ablssud kilonova candidates, the optical afterglows of GRB221009A and GRB 230812B, supernova SN2023wrk, and the possible optical counterpart of the neutrino event IceCube-240327B - 4FGL J0555.9+0030. Additionally, Lisnyky-GRANDMA team members O. Pyshna, A. Simon, and V. Vasylenko served as follow-up advocates, managing and organizing observations of particularly interesting events. As a result, the team members have co-authored seven GRANDMA papers and a multitude of GCN circulars.

LNM-SNClass - Large Number of Models Supernova Classifier

O. Pyshna[1], V. Morozov[2], A. Baransky[1]

[1]Astronomical Observatory of Taras Shevchenko National University of Kyiv, Ukraine
[2]KU Leuven, Belgium

Photometric classification of transients is a dynamically progressing field in astronomy, developed to find a way to classify transient objects based on photometric data, as spectroscopic results are not always available. Currently, the most used approach to photometric classification involves machine learning, however, in this work, we propose our method for classifying supernovae by types, involving Bayesian inference model fitting. The method is called: LNM-SNClass - Large Number of Models Supernova Classifier, which can be used to classify confirmed supernovae by types and can refine the classification results of a neural network to classify objects of unknown nature.

LNM-SNClass uses 195 supernovae models implemented in the SNCosmo package for SN Ia, Ib/c, Ib, Ic, Ic-BL, II, IIP, IIL, IIn, IIb, IIIpop types. Most of the models use three parameters to describe a light-curve shape – time offset, amplitude, and redshift except for salt2, in addition to having stretch and color parameters. At the end of the fit of all models to the object with a nested sampler, the code provides the values of three scores: log_likelihood, log_evidence, and AIC for each analyzed model. Consequently, exponentiated model scores are summed into three main types: Ia, Ib/c, and II resulting in a softmax probability for each.

As of now, tests are being made on objects with assumed known redshift and objects with calculated photometric redshift by our code, using ZTF r and g photometry of spectroscopically confirmed supernovae with known types to determine the accuracy of the proposed classifier. Our tests on around 2000 objects with different amounts of data points per object starting from 10 data points demonstrated >85% general accuracy, with completeness: 84%, 87%, 79%, purity: 92%, 81%, 78% with spectroscopic redshift, and >83% general accuracy, with completeness: 80%, 87%, 62% , purity: 88%, 68%, 75% with photometric redshift for type II, Ia and Ib/c respectively.

SOLAR PHYSICS
AND SOLAR ACTIVITY

Calculation of the total sunspots area based on the visible range observations

O.A. Baran, A.I. Prysiazhnyi, I.Ya. Pidstryhach

Astronomical Observatory of Ivan Franko National University of Lviv
Lviv, Ukraine

New methods for calculating the areas of particular structures in the solar atmosphere, which are manifested in images obtained in the visible spectral range, are proposed. The sunspot areas were calculated based on a set of images of the Sun obtained by the photoheliograph of the Astronomical Observatory of Ivan Franko National University of Lviv and on the data from the Solar Dynamics Observatory. All calculations were performed both for the total areas of the sunspots observed on the visible hemisphere of the Sun at a particular time and separately for their umbrae and penumbrae.

We reproduced the changes in sunspot areas during the period 2012-2023, which includes the period from the maximum phase of the 24th solar activity cycle to the moment of approaching the maximum of the 25th cycle, which is currently underway. We analyzed the changes in the ratio between the areas of umbrae and penumbrae of the sunspots with the phases of the solar cycle.

We compared our results with the data from the SolarMonitor project and found a high level of correlation between these datasets.

On specifying the amplitude of the 25th cycle of solar activity based on the rate of change of sunspots during the cycle growth phase

V.M. Efimenko, V.G. Lozitsky

Astronomical Observatory of the Taras Shevchenko National University of Kyiv, Ukraine

We previously proposed a prediction of the amplitude of cycle 25 of solar activity based on data analysis of previous solar cycles (https://doi.org/10.1016/j.asr.2023.04.006). For this, the dependence of the amplitude of 24 previous cycles on the rate of change in the number of sunspots during the growing phase of 11-year cycles was constructed. At the same time, the assessment of the forecasting quality was made on the

basis of correlations between the calculated and forecasted values. When determining the rate of change in the number of sunspots, the duration of the growth phase interval used for this was varied. The optimal interval obtained in the study was equal to 35 months, and the amplitude of the 25th cycle is expected at the level of W_{max} (25) = 150 units, which corresponds to the average power of the solar cycle, with a good implementation of the Hnievyshev-Ohl rule.

As it follows from the performed work, an important role belongs to the correct assessment of the rate of change in the number of spots in different cycles. We considered changes in the speed of the number of spots during the growth phase of solar cycles. It was found that part of the cycles has a monotonic growth curve (2/3 of the cycles), and the rest - non-monotonic. This requires making changes to previously obtained results. It should be mentioned that the author of a similar study, Pesnell W.D., Solar Physics, 2024 (https://doi.org/10.1007/s11207-024-02256-4), used part of the data on solar cycles (16 of 24). In the mentioned work, a forecast of 25 cycles of W_{max} (25) = 130 ± 0.5 was obtained, which is a fairly good result, although with implausibly high accuracy. New data on solar activity obtained over the past few months indicate that the 25th cycle can be classified as one-third of the cycles that have a non-monotonic growth curve. In this case, we can use the corresponding correlation dependence for such cycles and conclude that the median value corresponds to W_{max}(25) = 170. That is, even in the case of a non-monotonic growth curve of the 25th cycle, this cycle is expected average in power, similar to cycle No. 15 (1913-1923), which had W_{max}(15) = 175.7. However, until now, the non-monotonicity of the growth curve of the current cycle was not as contrasted as it was in the 15th cycle. Given this, we are inclined to another prediction as more realistic, namely W_{max} (25) = 140-150.

Modelling hard X-ray emission in individual solar flares

M. Gordovskyy

Centre for Astrophysics, University of Hertfordshire, UK

Test-particle approaches are widely used to investigate kinetics of energetic particles in the solar corona, and predict their observational manifestations, such as hard X-ray (HXR), microwave and low-frequency radio emissions. We use non-linear force-free magnetic field extrapolations obtained before several solar flares to model trajectories of particles in the solar corona. It is

demonstrated that cross-field drift can substantially affect trajectories of energetic electrons, and the locations where energetic electrons reach the chromosphere, producing HXR footpoint sources. This effect is particularly significant for particles moving in the vicinity of reconnecting current sheets. We conclude that magnetic connectivity alone cannot be used to predict the location of HXR footpoint sources, and, therefore, as a minimum, test-particle models of energetic electron kinetics must include the parallel motion and the ExB drift.

Dependence of strong magnetic field measurements in the solar atmosphere on the techniques used

M.A. Hromov[1], I.I. Yakovkin[2], V.G. Lozitsky[2]

[1]Faculty of Physics of the Taras Shevchenko National University of Kyiv, Ukraine
[2]Astronomical Observatory of the Taras Shevchenko National University of Kyiv, Ukraine

Strong magnetic magnetic fields in the solar atmosphere are most reliably measured by the Zeeman effect when the filling factor is close to unity and the magnetic splitting of the spectral components of the magnetosensitive line is complete. The latter is called the strong field regime in solar magnetometry. In fact, this mode can be observed only at the level of the photosphere, in sunspots, and in lines with large Lande factors. For measurements in the chromosphere and especially the solar corona, it is necessary to use another mode, a weak field approximation (WFA), in which the visible Zeeman splitting is much smaller than the observed half-width of the spectral line. In this case, when the filling factor is close to unity, the longitudinal component of the magnetic field is measured, and when it is small, in the first approximation, the product of the local field by the filling factor is measured. Obtaining the actual field values in this case is quite difficult and not always unambiguous. One of the methods used by the authors is based on the analysis of the shape of the profile bisectors (see, e.g., https://link.springer.com/article/10.3103/S0884591323050070). This method sometimes leads to field values that are even greater than those observed in sunspots by the direct method. The reality and the upper limit of local fields with this approach represent an understudied problem. In the report, we plan to provide and discuss some specific details in this problem.

Anti-Hale solar active regions with high flaring activity

N.N. Kondrashova[1], V.N.Krivodubskij[2]

[1] Main Astronomical Observatory, National Academy of Sciences of Ukraine, Kyiv, Ukraine
[2]Astronomical Observatory of Taras Shevchenko National University of Kyiv, Ukraine

It is generally accepted that the magnetic field of most active regions are generated by a global dynamo. Bipolar active regions are formed by a toroidal magnetic field, which is generated from a poloidal field through differential rotation. They obey the laws of the global dynamo, Hale's law of polarities and Joy's law of the axis of the active region. However, a few percent of active regions do not obey the laws of the global dynamo. The orientation of the magnetic polarities of these regions is different from the location of the polarities of other (regular) sunspots in the same hemisphere. The mechanism of the processes contributing to the appearance of anti-Hale active regions is not yet fully known.

According to observations, a tendency of abnormal active regions to have increased flaring activity is noticeable. Coronal mass ejections and radiation from the powerful flares cause the magnetic storms, blackouts, disruption of the technical systems. The storms affect the weather and the people's health. For the development of forecasting methods, it is important to study the evolution of these regions, flaring activity, and properties of their magnetic field.

We have analyzed the evolution and flaring activity of anti-Hale active regions NOAA 12673, NOAA 10930 and NOAA 13536. They produced many flares, coronal mass ejections and jets. Their magnetic field poles were rotated 90 degrees compared to other active regions. We used data from space observatories. The full-disk magnetograms, continuum images and EUV-images were provided by the Solar Dynamics Observatory (SDO) the Helioseismic and Magnetic Imager (HMI) and the Atmospheric Imaging Assembly (AIA). The X-ray data were obtained at Geostationary Operational Environmental Satellite (GOES).

The active region NOAA 12673 was observed in the solar disk from 29th of August to 10th of September 2017 in the phase of decline of the 24th solar cycle. The structure of the region was changing. The number and area of spots increased.The complexity of the magnetic field was increasing rapidly. The active region studied produced the flare X9.3-class on 6th of September 2017, which was included in the list of the most power flares

since 1976. The flare caused a CME and a strong shortwave radio blackout over Europe, Afrika and the Atlantic Ocean and a strong geomagnetic storm. The active region erupted again on September 10th, producing a powerful flare X8-class, which caused a shortwave radio blackout over the Americas. It was a ground level event. The energetic protons were accelerated by the explosion toward the Earth.

The active region NOAA 10930, which was observed in the decline phase of the 23th cycle, produced the flare X9.0-class. This flare was included in the list of the most power flares also.

The active region NOAA 13536 appeared in the solar disk on December 31, 2023 in the growth phase of 25th cycle. It erupted with the flare X5-class, which was the strongest since September 2017.

A possible mechanism contributing to the appearance of the NOAA 12673, NOAA 10930 and NOAA 13563 anti-Hale active regions is discussed. We assume that the emergence of these regions was associated with the accidental changes in the turbulent dynamo regime in the SCZ. In particular, the detected magnetic anomalies in NOAA 12673 and NOAA 10930 (observed in the decline phase of the 23th and 24th cycles) may indicate the influence of the diffusion dynamo on the evolution of these regions, since this source of small-scale magnetic fluctuations gives the most noticeable contribution to the surface magnetism near the minima of the cycles.Considering the tendency of anomalous active regions to increase flare activity, the further study of the active regions, which are characterized by violations of Hale's and Joy's laws, becomes relevant.

Solar faculaes and flocculi: observations and modelling

R.I. Kostik

Main Astronomical Observatory of National Academy of Sciences, Kyiv, Ukraine

The results of spectropolarimetric and filter observations of a facula area located near the solar disc center in the lines FeI 1564.3 nm, FeI 1565.8 nm, BaII 455.4 nm and CaII H 396.8 nm are discussed. The observations were performed at the German Vacuum Tower Telescope of the Observatorio del Teide (Tenerife, Spain). The power of oscillations of velocity depending on the frequency of oscillations at heights of h = 0 km - 1600 km in the atmosphere of the Sun and the dependence of the contrast in the center of the CaII line (h = 1600 km) on the tension of the photosphere magnetic field

(h = 0 km) are discussed. The results of observations are compared with the 3d-dynamic model of the atmosphere of the Sun.

Electrical conductivity and magnetic permeability in the turbulent layers of the Sun

V. N. Krivodubskij

Astronomical Observatory of Taras Shevchenko National University of Kyiv, Ukraine

Over the last 50 years, the Astronomical Observatory of the Taras Shevchenko Kyiv National University has been conducting research on the restructuring of the global magnetism of the Sun within the framework of macroscopic magnetohydrodynamics, in which the turbulent motions of plasma play a key role. The peculiarity of the new approach is that turbulence, contrary to popular belief, does not always destroy large-scale magnetic structures, but under certain conditions can create them. With this in mind, we have calculated the electrodynamic parameters of the plasma (which determine the reconstruction of global magnetism) in the turbulent layers of the Sun. As a result of the calculations for the models of the photosphere and the solar convective zone (SCZ), the distributions along the solar radius of the coefficients of kinematic ν, magnetic ν_m and turbulent ν_T viscosities, hydrodynamic Re and magnetic Rm Reynolds numbers, gas-kinetic σ and turbulent σ_T electrical conductivities and turbulent magnetic permeability μ_T were determined. The values of the calculated parameters are in the following ranges: $\nu \approx 0.2 - 10\ cm^2/s$, $\nu_m \approx 6x10^8 - 8x10^2 cm^2/s$, $\nu_T \approx 10^{11} - 10^{13}\ cm^2/s$, $Re \approx 5x10^{11} - 5x10^{13}$, $Rm \approx 10^4 - 10^{10}$, $\sigma \approx 10^{11} - 4x10^{16}$ CGS, $\sigma_T \approx 10^9 - 4x10^{11}$ CGS, $\mu_T \approx 10^{-2} - 4x10^{-5}$. It is relevant that the turbulent electrical conductivity σ_T was significantly smaller than the gas-kinetic conductivity σ, and the turbulent magnetic permeability μ_T was significantly smaller than the gas-kinetic value $\mu = 1$. The spatio-temporal evolution of the global magnetism of the Sun is analyzed taking into account these turbulent parameters. Since the conditions $\sigma_T << \sigma$, $\mu_T << 1$ are fulfilled everywhere in the turbulent layers, the value of the turbulent magnetic diffusion parameter $D_T = c^2/4\pi\sigma_T\mu_T$, calculated by, us turned out to be 4 to 9 orders of magnitude higher than the magnetic viscosity coefficient $\nu_m = c^2/4\pi\sigma$, responsible for the ohmic dissipation of magnetic fields. As a result, it becomes possible to

theoretically explain the rapid observed reconstruction of magnetism of the Sun. The radial inhomogeneity of the turbulent viscosity ν_T and the condition $\mu_T << 1$, revealed by us, testify to the strong macroscopic diamagnetism of the turbulent layers of the Sun. Macroscopic turbulent diamagnetism in deep layers of the SCZ plays the role of negative magnetic buoyancy. As a result, it contributes to the formation of a magnetic layer of a steady state toroidal magnetic field with a strength of about 3000–4000 G near the bottom of the SCZ.

Magnetic fields in the main sunspot of the active region NOAA 13372

N.I. Lozitska

Astronomical Observatory of the Taras Shevchenko National University of Kyiv, Ukraine

The peculiarities of the magnetic field distribution in the plane of a large sunspot measured by the Zeeman splitting of five photospheric lines with a different formation height are presented. The spectrogram of the spot was obtained by V. Lozitsky at the HST of AO KNU on July 17, 2023. The processing of the spectra using the program of I. Yakovkin showed that the magnetic field module in the sunspot umbra reached 2600 G. No signs of stronger magnetic fields were found in this sunspot. The longitudinal component of the magnetic field in the FeI 6290.97, FeI 6297.80, and TiI 6303.76Å lines was 80-99% of the value of the magnetic field modulus, and in the FeI 6301.52, FeI 6302.51 lines it was only 65-75%. The value of the magnetic field module by named photospheric lines slightly decreases with the height in the atmosphere.

Comparison of magnetic fields and Doppler velocities in an X-class solar flare as measured by D1, D2, D3, H-alpha, and NiI 5892.9 lines

V.G. Lozitsky, I.I. Yakovkin, N.I. Lozitska

Astronomical Observatory of the Taras Shevchenko National University of Kyiv, Ukraine

The main goal of our research is to estimate the upper magnetic field limit in a flare using direct observations in spectral lines formed in a wide range

of height – from the photosphere to the transition region between the chromosphere and corona. Our method is based on Stokes V spectro-polarimetry of D1, D2, D3, H-alpha, and NiI 5892.9 lines and the nearest spectral continuum with a total spectral range of approximately 50 Å. The object of the study is an area of the solar flare on 17 July 2004 of the X1.1/2N class which arose in active region NOAA 10649. The main results of our study are the following: (a) the maximum magnetic field strength measured in the flare directly from the splitting of the line profiles reached 4.7–6.0 kG by the D1 and D2 lines, 1.9 kG by the D3 line, and only 0.6 kG by the H-alpha and Ni I lines; (b) Doppler (longitudinal) velocities changed sign with height in the atmosphere and were within the –4.5 to 7.7 km/s range; (c) observational indications of stronger magnetic fields (> 6 kG) were not found when studying wide spectral intervals (up to 15 angstroms) around the H-alpha and D3 lines. On the basis of these results, it can be concluded that in the studied solar flare there was a significant altitudinal heterogeneity of the magnetic field and Doppler velocities, and the peak values of the magnetic field in the chromosphere (6 kG) were greater than in the nearest sunspots at the photospheric level (2.8 kG). This indicates, likely, a local strengthening ("collapse") of the magnetic field in the region of the solar flare. The latter is confirmed by the fact that the Doppler velocities in the chromosphere had the opposite signs and can indicate the concentration of matter and magnetic field at this level in the atmosphere.

Height of the solar polar chromosphere in 2012–2024

S.M. Osipov, M.I. Pishkalo

Main Astronomical Observatory of the National Academy of Sciences of Ukraine

Based on the results of many years observations in the H_a line in 2012–2024, the height of the solar polar chromosphere in 2012–2024 was determined as a difference in the position of the maxima of radial brightness gradients in the continuum and in the H_a line core. It is shown that the height of the polar chromosphere decreases during periods of high solar activity (~4500 km or ~6.3") and increases during periods of quiet Sun (~5000 km or ~6.9"). A strong north-south asymmetry of the results in 2016–2017 was revealed, which is likely associated with the dynamics and magnitude of polar magnetic fields in the 24th solar cycle. It has been

obtained that there is a strong correlation between the average height of the polar chromosphere and the strength of the polar magnetic field (according to data from the Wilcox Solar Observatory). The correlation coefficient between the average height of the polar chromosphere and the average values of the modulus of the polar magnetic field strength is was calculated to be becomes 0.87 for the northern hemisphere and 0.53 for the southern hemisphere (last value increases to 0.77 with time shift +1 year).

Motion features of chromospheric plasma in the magnetic loops of arch filament system

M.M. Pasechnik

Main Astronomical Observatory, NAS of Ukraine, 27, Zabolotnoho Str., 03143 Kyiv, Ukraine

We study the chromospheric plasma dynamics in two magnetic loops of an arch filament system (AFS), which was formed on a site of active region NOAA 11024. This AO site (its length was 10 Mm) was located in the area of emergence of a new serpentine magnetic flux in the form of ascending loops. The characteristic configuration formed by these magnetic loops is referred to as AFS. As a result of repeated reconnection between the serpentine loops and the surrounding pre-existing magnetic field AO, chromospheric plasma flows occur in them — Hα-ejections. On the studied site there was also a pore and at a distance of about 7.2 Mm from it under the AFS an Ellerman bomb developing. We investigated in detail the formation and development of Hα-ejections that formed in two magnetic loops during our observations. For this were analyzed spectral data with a high spatial (~ 1") and temporal (about 3 sec) resolution were obtained with Franch-Italian solar telescope THEMIS (Tenerife, Spain) on July 4, 2009. The observation time was 20 minutes (to 9^h52^m – 10^h11^m UT). Used the spectral region that containing the central part of the Hα chromospheric line.

In all spectra, Hα-ejections (surges) were visible in the absorption. Changes of the Stokes I profiles shape were studied - they were very diverse. Depending on whether the ejection moved to the upward or to the downward, the component of the profile corresponding to it was projected onto the blue or red Hα line wing. Doppler shifts of the profile components were used to calculate the line-of-sight velocities (Vlos) along the cross-

section of the surge jets at the place of their maximum intensity. Changes in Vlos of jets movement in the magnetic loop and their movement direction depended on the magnetic field structure and the phase of surge development. The Vlos values in the site without active formations did not exceed ±2 km/s. It was found that surges can consist of several jets that were formed during successive and periodic magnetic reconnections. Most of the Vlos change curves consisted of several segments. This indicates that the large jets were composed of several smaller jets, i.e. they had a fibrous structure.

One of the studied loops already existed at the beginning of our observations. In it, a jet with an upward plasma movement was observed, in which the Vlos along the cross section varied from -70 to -86 km/s. During our observations, three more jets were formed in this loop - two with an upward movement of matter and one with a downward movement. Their average Doppler velocity at first appearance were -62, -45 and 53 km/s, respectively. The second of the studied magnetic loops emerged during our observations. A surge developed in it with a low intensity, but with a Vlos close to -90 km/s. Its intensity gradually increased and eventually became greater than the intensity of the main profile of the Hα line. Gradually, the upward velocity plasma decreased and the direction of movement changed to the opposite. Probably, the substance of the jets reached a certain height or the tops of the magnetic loops along which it rose and began to move downwards under the influence of gravity. The Vlos of the downward movement gradually increased. It should be noted that the plasma moved along the magnetic loop unevenly - sometimes slowing down, then speeding up.

Our work is based on a detailed study of observational data that was obtained with high spatial and temporal resolution, it allowed us to better understand the features of the formation and development of surges that formed in AFS magnetic loops. Furthermore, as correctly pointed out in a recent paper, studies of ejected pulsed plasma using high-resolution Hα-spectroscopy are performed infrequently, and we still have little knowledge about the spectral characteristics of surges. The new observational data for Hα-ejections obtained in our work can be used to verify existing and create new theoretical models.

Rating of extreme space weather events based on geomagnetic data, variations of cosmic rays and radio astronomical observations

M. I. Ryabov[1], A. L. Sukharev[1], M. I. Orlyuk[2], Yu. P. Sumaruk [2], A. Romenets [2], D. M. Ryabov[3]

[1]Odesa observatory "URAN-4" RI NANU
[2]S.I. Subbotin Institute of Geophysics NAS of Ukraine
[3]Odesa State University of Intellectual Technologies and Telecommunications

The extreme G5 class geomagnetic storm that occurred from May 10 to May 14, 2024 aroused particular interest in similar events in the solar cycle. First of all, it should be noted the special nature of the manifestation of activity in the 25th cycle, which distinguishes it from the previous ones. Until now, both solar hemispheres have shown increased activity almost quasi synchronously. As a result, the total values of the Wolf numbers for both hemispheres exceeded those of the previous 24 cycles. A distinctive feature of the current solar cycle is also a significant number of M and X-class flares, many of which were quasi-synchronous even in different hemispheres.

Based on the data of the catalogues of ionospheric and magnetic storms, information on the events of forbush descents of cosmic rays and the catalogue of magnetic storms in the Odessa Magnetic Anomaly, a rating of extreme manifestations of space weather for the period from 1987 to the present has been compiled.

This period corresponds to the program for monitoring the fluxes of powerful space radio sources carried out on the radio telescope «URAN-4» RI NANU , which react to changes in space weather.

Advancing Understanding of Small-scale Chromospheric Dynamics Using GST Data

Vasyl Yurchyshyn

Big Bear Solar Observatory, New Jersey Institute of Technology

Large- and small-scale jets and upflows observed in the lower atmosphere of the quiet Sun (QS) are thought to play an important role in the transfer of

mass and energy from the dense chromosphere into the corona. Type II spicules and their disk counterparts, rapid blue and red shifted excursions (RBEs and RREs), are a subset of the small-scale phenomena discovered in off-limb Hinode data. Although their origin may affect the corona by generating shocks, flows, waves, and electric currents, their detailed physical cause and role in providing mass and energy to the corona remain largely unknown.

In this presentation I will discuss recent progress in studying type II spicules facilitated by data from the Goode Solar Telescope (GST). Spectral measurements of various RBE and RRE events as well as explorations of the topology of the magnetic field environment hosting those features all seem to indicate that these events result from magnetic reconnection driven by rapidly varying small-scale magnetic fields present in highly turbulent solar photosphere.

Particle transport effects derived in a few solar flares with sunquakes in cycle 25

V. Zharkova[1,2] and S. Zharkov [2,3]

[1] Northumbria University, MPEE, Newcastle-Upon-Tyne, United Kingdom;
[2] ZVS Research Enterprise Ltd., London, United Kingdom;
[3] University of Hull, Physics and Mathematics, Hull, United Kingdom

We investigate five solar flares with sunquakes observed on the solar disk in 2021-2023 and their emission in multiple wavelengths. These results are interpreted by the simulation of accelerated particle transport into flaring atmosphere considering collisional and Ohmic mechanisms of energy losses with return current and diffusive pitch-angle scattering in converging magnetic field. We also consider a hydrodynamic response of the ambient plasma to the heating by energetic particles and also a hydrodynamic response of the solar interior to propagation of supersonic shocks. Various combinations of the modelling results are tested for each flare with sunquakes to derive most probable scenario of particle precipitation leading to the observed signatures in HXR, EUV, optical and seismic emission.

ENSO Index Variations and Links with Solar and Volcanic Activity

V. Zharkova[1,2] and I. Vasilieva [2,3]

[1] Northumbria University, Newcastle upon Tyne, UK
[2] ZVS Research Enterprise Ltd., London, UK
[3] Main Astronomical Observatory, National Academy of Sciences
Kyiv, Ukraine

In this paper, we investigated the Oceanic Niño Index (ONI), for simplicity called in this paper an El Nino Southern Oscillation (ENSO) index in 1950-2023 by applying the wavelet spectral transform and the IBM SPSS correlations analysis. ONI follows the three months' current measurements of the average temperature of the sea surface in the East-Central tropical part of the Pacific Ocean nearby the international line of the date change over the average sea surface temperature over the past 30 years. The ENSO index is found to have a strong (>87%) correlation with the Global Land-Ocean Temperature (GLOT). The scatter plots of the ENSO-GLOT correlation with the linear and cubic fits have shown that the ENSO index is better fit by the cubic polynomial increasing proportionally to a cubic power of the GLOT variations. The wavelet analysis allowed us to detect the two key periods in the ENSO (ONI) index: 4 - 5 years and 12 years. The smaller period of 4.5 years can be linked to the motion of tectonic plates while the larger period of 12 years is shown to have a noticeable correlation of 25% with frequencies of the underwater (submarine) volcanic eruptions in the areas with ENSO occurrences. Not withholding any local terrestrial factors considered to contribute to the ENSO occurrences, we investigated the possibility of the volcanic eruptions causing ENSO to be also induced by the tidal forces of Jupiter and Sun showing the correlation of the underwater volcanic eruption frequency with the Jupiter-Earth distances to be 12% and with the Sun-Earth distances, induced by the solar inertial motion, in January, when the Earth is turned to the Sun with the southern hemisphere where the ENSO occurs, to become 15%. Hence, the underwater volcanic eruptions induced by tidal forces of Jupiter and Sun can be the essential additional factors imposing this 12 year period of the ENSO (ONI) index variations.

ATMOSPHERE AND IONOSPHERE RESEARCH

Magnetic-ionospheric disturbances during solar eclipse of October 25, 2022 over Ukraine

L.F. Chernogor, V.O. Bessarabova

V.N. Karazin Kharkiv National University, Kharkiv, Ukraine

The near-Earth environment, which is part of the Earth–atmosphere–ionosphere–magnetosphere (EAIM) system, is the main functioning radio channel. It is used by radio communications, radio navigation, radar, remote sensing, and radio astronomy systems. The EAIM system and radio channel are rarely in a quiet state. From time to time they become disturbed by high energy sources. One of them is a solar eclipse (SE). Although the disturbance of the EAIM system by a solar eclipse has been studied for more than a hundred years, the study of the entire set of effects in this system remains an urgent task. This is due to the fact that the effects of an SE significantly depend on the eclipse magnitude, the state of space weather, position in the solar activity cycle, time of year, time of day, geographic coordinates, etc. All this determines the relevance of studying the response of the EAIM system and geophysical fields to each new SE.

The aim of this paper is to describe the results of the study of temporal variations in the components of the geomagnetic field and total electron content (TEC) in the ionosphere that accompanied the partial SE on October 25, 2022 over Ukraine.

The SE of Saros 124 was observed on October 25, 2022 in Europe, the Middle East, Central Asia, western Siberia, and northwestern Africa. The SE started in Iceland (geographic coordinates are: 66°28′N, 18°57′W) at 08:58:20 UT, and ended in the Arabian Sea area with coordinates of 17°35′N, 66°31′E at 13:02:16 UT (UT is Universal Time). The largest magnitude of the partial SE, equal to 0.8623, was observed in the area with coordinates 61°36′N, 77°24′E. On the territory of Ukraine it did not exceed 0.53–0.73, and the relative obscuration area of the solar disk was 43–66%.

To correctly identify the effects of an SE, a thorough analysis of the state of space weather is required. Note that on October 25, 2022, on the day of the SE, the space weather state was undisturbed and quite favorable for observing the geomagnetic and ionospheric effects of the SE. At the same time, the days from October 21 to October 24, 2022 were somewhat disturbed. Therefore, October 20 and October 26, 2022 were chosen as reference days.

The registration results of *X*-, *Y*- and *Z*-components of the geomagnetic field at the Lviv station and the results of measuring the parameters of radio

signals from the Global Navigation Satellite System in Kharkiv were used as initial data. Temporal resolution was 1 min. The error in measuring the level of geomagnetic components is 0.1 nT, and for TEC it is 0.1 TECU.

The main results of the study are as follows. The SE over Ukraine caused aperiodic disturbances in the components of the geomagnetic field, which reached 2–3 nT. The greatest disturbance was observed in the *X*-component, and the smallest in the *Z*-component. The duration of the disturbance was 80–100 min. The SE was accompanied by quasi-periodic disturbances of the geomagnetic field components. The amplitude of oscillations with a period of 30±5 min and a duration of 70–80 min reached 2 nT. The SE caused a decrease in TEC from ~24 to ~18 TECU. The delay time of the TEC response to the SE was about 14 min. On average, the linear recombination coefficient was close to $1.2 \cdot 10^{-3}$ s^{-1}. The results of the assessment of magnetic and ionospheric effects are in good agreement with the observational results.

The study was partially supported by State Budget grant provided by the Ministry of Education and Science (registration no. 0122U001476).

The vertical ozone profiles over the Faraday/Vernadsky station, Antarctic Peninsula: peculiarities and trends

Yu. Andrienko[1], A. Grytsai[1], G. Milinevsky[2,3], J. Shanklin[4], Y. Shi[3], R. Yu[3], O. Poluden[5], O. Ivaniha[6]

[1]Physics Faculty, Taras Shevchenko National University of Kyiv, Kyiv, Ukraine
[2]Main Astronomical Observatory of NAS of Ukraine, Kyiv, Ukraine
[3]College of Physics, ICFS, Jilin University, Changchun, China
[4]British Antarctic Survey, Cambridge, United Kingdom
[5]National Antarctic Scientific Center of Ukraine, Kyiv, Ukraine
[6]Earth Physics and Astrophysics Department, Universidad Complutense de Madrid, Madrid, Spain

Data from the original series of ozone observations over the Faraday/Vernadsky Antarctic station since 1973 have been processed. The ozone profiles in this unique series of observations cover the period before the ozone hole time and in the period of the ozone hole. Approximately 1200 observations made by the Umkehr method on a Dobson spectrophotometer were processed using the UMK92 ozone profile retrieval

algorithm. In the period before the ozone hole of 1973–1983, the partial ozone column at the maximum of ozone profiles varies from 134 to 56 DU layer^{-1} with a profile maximum height of 14–18 km. The rate of change of the total value of the ozone column above the station and the shape of the vertical distribution of ozone during the existence of the ozone hole were analyzed. The station's location at the edge of the ozone hole area causes the variation in profiles. An analysis of vertical ozone distribution during the ozone hole was carried out. Most ozone profiles exhibit two maxima that are reasonably symmetrical relative to the zone of a significant reduction in ozone partial column, located at the 15–17 km altitude and has an ozone value of 20–25 DU layer^{-1}. These maxima's ozone partial column value does not exceed 40 DU layer^{-1}. Profiles are asymmetric concerning the area of minimum concentration, which is higher for them (20 km long), were also obtained. Based on the data of 50 years of observations, the trends in ozone profiles in the atmosphere above the Faraday/Vernadsky station from the time before the appearance of the ozone hole at the heights corresponding to the levels of the tropopause, stratopause and at the level of the highest ozone concentration were constructed and analyzed. Observations from 1957 to 1972 based on the data of the British Antarctic Survey were also considered [1].

[1] Farman, J.C., Hamilton, R.A. 1975. Measurements of atmospheric ozone at the Argentine Islands and Halley Bay, 1957-72. Cambridge, British Antarctic Survey, 40pp. (British Antarctic Survey Scientific Reports, 90).

Effects from the 23–24 April 2023 geospace storm over the People's Republic of China

L.F. Chernogor[1,2,3], Y.H. Zhdanko[2], Q. Guo[3], Y. Zheng[1], J. Wang[4,5,6]

[1]College of Electronic Information, Qingdao University, Qingdao, China
[2]V.N. Karazin Kharkiv National University, Kharkiv, Ukraine
[3] Harbin Engineering University, Harbin, China
[4]School of Microelectronics, Tianjin University, Tianjin, China
[5]Tianjin University, Qingdao, China
[6]Shandong Engineering Technology Research Center of Ocean Information Awareness and Transmission, Qingdao, China

The study of a variety of physical effects accompanying geospace storms still remains an urgent need. There are a few reasons for this. First, each

storm has individual, in addition to general, characteristics. Second, the manifestation of geospace storms depends on the specifics of the solar storm, solar cycle phase, season, local time, and the geographic coordinates of the observation site. Third, the manifestation of geospace storms depends on diagnostics employed to study the disturbances arising in various geospheres and geophysical fields. Important information on the processes operating in the ionosphere during geospace storms is provided by observations at oblique incidence. In addition, these systems are capable of measuring not only ionospheric parameters, but also the characteristics of high-frequency (HF) radio waves. Variations of space weather significantly affect the propagation of radio waves of all bands, and this is especially true for HF radio waves. The basic cause of variations in space weather is solar storms and their consequences, geospace storms.

The purpose of this report is to present the results of observations of temporal variations in the characteristics of HF radio waves and ionospheric disturbances over the 23–24 April 2023 geospace storm period and on the reference days via the multifrequency multiple path software-defined radio system for HF probing the ionosphere at oblique incidence.

This radio system is located at the Harbin Engineering University, the People's Republic of China. It continuously monitors the states of the ionosphere and thirteen HF communication links. The current state of the ionosphere was assessed utilizing the ionosonde nearest to Harbin, which is located in Japan at the city of Wakkanai. To check disturbances in the geomagnetic field, the data with 1-min temporal and 1-nT amplitude resolutions were retrieved from the INTERMAGNET observatories.

For the first time, a detailed comprehensive analysis of variations in the space weather state and the characteristics of HF radio waves caused by one of the strongest storms in the 25th solar cycle was carried out. The components of the geospace storm, namely, the magnetic and ionospheric storms, were determined to be recurrent. The moderate geospace storm was accompanied by superstrong magnetic storms and severe and strong ionospheric storms. The ionospheric storms were both negative, with negative ionospheric indexes I_{NIS} of 6.6 and 4.0. Significant perturbations were observed in radio wave characteristics in the 5- to 10-MHz frequency range and in ionospheric parameters between ~130- and 260-km altitude, via the multifrequency multiple path software-defined radio system for oblique incidence sounding. Not only did the parameters of a regular ionosphere were significantly disturbed, but wave activity in the magnetic field, atmosphere, and the ionosphere on 22 and 23 April 2023 also considerably increased, especially in the 100–120-min period range. This indicates a synergetic coupling between the geospace storm components.

The slow quasi-periodic processes in the ionosphere (characteristic times of ~100–120 min) acted to shift the radiowave reflection level by 30–130 km at an average speed of ~10–60 m/s, depending on the propagation path. Short-term reflection level shifts of 30–70 km occurred at an average speed of 50–100 m/s over a span of ~10 min. The amplitude of perturbations in the electron density with 8–15-min to 40-min periods varied from 1.6–3.5% to 29–39%, respectively.

About reliability control of polarimetric clear sky measurements

O.S. Ovsak

Main Astronomical Observatory, National Academy of Sciences of Ukraine, Kyiv, Ukraine

Polarization characteristics of radiation scattered by the Earth's atmosphere are formed by the interaction of sunlight with its gas and aerosol components. These characteristics can be determined using spectropolarimeters installed on ground boards, on airplanes and on artificial satellites of the Earth. According to the results of such measurements, spatial distributions of polarimetric parameters of light scattered by the atmosphere were calculated: degree (DoLP) and angle (AoLP) of linear polarization, of which the probable characteristics of atmospheric aerosols were determined.

In particular, a special analysis of the phase dependencies of the DoLP parameter at different wavelengths in the visible range, obtained with a clear sky above the Earth's position, allows us to determine the main modes of atmospheric aerosols and their characteristics. However, the results of polarimetric measurements can be significantly distorted by errors in the organization of the place or conditions of observation, as well as neglect of the influence of extraneous objects and processes. According to numerous studies, the spatial distribution of the AoLP parameter on the celestial hemisphere is resistant to significant changes in the aerosol component of the Earth's atmosphere. Therefore, to to control reliability of data from polarimetric measurements of clear sky, the spatial scheme of distribution of parameter AoLP calculated from the data of polarimetric measurements is proposed, compared with the model spatial distribution AoLP calculated in the theory of single Rayleigh scattering over the same site on the ground, for the exact time and date of measurement.

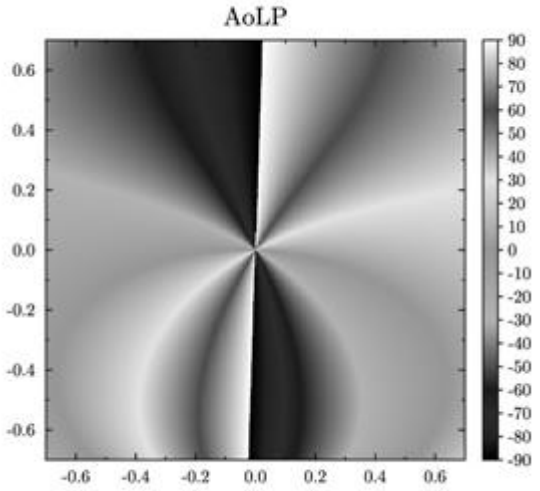

Fig. 1. Spatial configuration of the AoLP parameter in the sky above the observation site.

The Fig.1 shows a graphical view of the results of model calculations with a single Rayleigh scattering of the spatial configuration of the AoLP parameter of the sky above the site of the MAO NAS of Ukraine (Kyiv, Golosiev, 50°21'57.0"N, 30°30'02.3"E) as of 11:50 on October 31, 2022. The field of view of the image is 126° x 126° and can be changed according to the design field of view from the polarimetric data.

Infrasonic effect of the explosion of the Tonga supervolcano, registered at the Ukrainian Antarctic Akademik Vernadsky station

L.F. Chernogor[1], O.I. Liashchuk[2], M.B. Shevelev[1]

[1]V.N. Karazin Kharkiv National University, Kharkiv, Ukraine
[2]Main Center of Special Monitoring, Gorodok, Zhytomyr region, Ukraine

The study of infrasonic effects from high-energy localized sources is an urgent task from the point of view of solving problems of detection,

identification and selection of signals and their sources. For empirical model developing of the acoustic signals' propagation in heterogeneous media, it is important to reliably estimate the parameters of acoustic signals generated by powerful sources of natural and man-made origin.

One of these sources is the explosive eruption of the Tonga supervolcano (geographic coordinates: 20°54′S, 175°38′W). The event took place on January 15, 2022, in the time range from 04:00 to 05:00 UT. The peculiarity of this event was that the activity of the volcano manifested itself in several explosions. These explosions were followed by earthquakes, tsunamis, atmospheric shock waves, and a number of secondary effects in all subsystems of the Earth system such as internal shells, oceans, atmosphere, ionosphere, and magnetosphere. Tsunami waves were recorded in the Pacific and Indian oceans. Atmospheric waves have been recorded by instruments around the globe at least several times. The main parameters of the volcano are as follows: the thermal energy was $3.6 \cdot 10^{19}$ J, the blast wave energy reached $0.9 \cdot 10^{17}$ J, the volcano magnitude was equal to 5.5, the intensity was approximately 12.1, the mass of substance emissions was about 2.9 Gt, and emission products were recorded at an altitude of up to 58 km.

This report aims to describe the findings of an evaluation conducted on the parameters of acoustic effects, which were a result of the explosive eruption of the Tonga supervolcano. The data collection process was executed at the Ukrainian Antarctic Akademik Vernadsky station, located at the geographic coordinates: 65°15′S, 64°16′W. The infrasound signals were meticulously recorded by the K-304 acoustic station, which is equipped with a condenser-type microbarograph. The complex's parameters are as follows: it possesses a sensitivity of 1 Pa, a resolution equivalent to 1 Pa, and operates within a frequency band from 0.003 to 12 Hz. The distance from the source of the eruption to the station was approximately 8867 km.

The primary results of the analysis are as follows: Fluctuations in atmospheric pressure were launched by a shock wave that propagated in the Earth's atmosphere with an initial speed of approximately 1000 m s^{-1}. The first acoustic arrival was documented by microbarographs around 12:00UT. The speed of the wave front was approximately 315 m s^{-1}, the period extended to 450–500 s, the amplitude was around 275 ± 30 Pa, and the duration was about half an hour. These parameters are characteristic of a non-dispersive, non-absorpted Lamb wave. The second signal, induced by the infrasonic wave, had a longer duration and was recorded for 2.5 hours. During this time, the amplitude reached 70±9 Pa, the main period was about 10 and 100 s, and the speed fluctuated between 280 and 300 m s^{-1}.

Approximately 1.5 hours after the arrival of the first infrasonic signal, another group of infrasonic signals was recorded in the atmosphere. These were caused by the tsunami and exhibited the lowest speed (about 200 m/s) and an amplitude close to 20±3 Pa.

It has been confirmed that the explosive eruption of the Tonga supervolcano caused significant disturbances in the atmosphere and the World Ocean on an almost global scale. For the first time, atmospheric effects from infrasonic wave, and tsunami were identified, and their parameters were assessed.

The work was partially supported by a Ukraine state-funded research projects (grant no. 0122U001476, 0124U000461, 0124U000478).

Hydrometeorological risks according to the PERUN scenario of climate change in the Czech Republic

R. Tolasz[1], V. Šustková[1], A. Valík[1], I. Dvoretska[1,2]

[1]Czech Hydrometeorological Institute, Ostrava, Czech Republic
[2]Ukrainian Hydrometeorological Institute, Kyiv, Ukraine

The Czech Hydrometeorological Institute is the leading researcher of the PERUN project (TAČR, SS02030040), where one of the many goals is the preparation of climate change scenarios for the Czech Republic by the end of the century. We prepare the scenarios using the ALADIN climate model [1, 2] according to two socioeconomic emission scenarios, SSP2-4.5 and SSP5-8.5 [3]. We are preparing scenarios for selected climatological elements and characteristics in a model step of 2.3x2.3 km, not only within the borders of the Czech Republic but with an overlap beyond the borders so that we also cover the basins of the streams that bring surface water to our territory. Outputs from the climate model ALADIN-CLIMATE/CZ are aggregated into monthly and annual averages, extremes and indices for 2021–2040, 2041–2060, 2061–2080 and 2081–2100 years intervals. The basic climate elements included in our research are average, maximum, and minimum temperature, precipitation, air humidity, solar radiation, and wind speed. It is supplemented by selected, commonly used indices. To prepare adaptation measures and documents for other strategic documents within the Czech Republic, we are also preparing scenarios of hydrometeorological risks and their probable changes by the end of the century. Here, we mainly monitor the characteristics of drought, heat, frost, intense precipitation and fire weather. A geographic information system (GIS) is used for the spatial

analysis of this data and the subsequent creation of cartographic outputs, specifically the desktop version of the ArcGIS system from ESRI [4]. For the creation of raster maps, we use the CLIDATA-DEM interpolation method developed at the ČHMÚ [5]. This interpolation method considers the effect of altitude (or the orientation and inclination of slopes or landscape cover) on the interpolated quantity. It preserves the original measured value at a known point.

[1] Brožková, R., Bučánek, A., Mašek, J., Smolíková, P., Trojáková. 2019. Nová provozní konfigurace modelu ALADIN ve vysokém rozlišení. Meteorologické zprávy, 72, 5, 129–139. ISSN 0026-1173.

[2] Termonia, P., et al. 2018. The ALADIN System and its canonical model configurations AROME CY41T1 and ALARO CY40T1. Geosci. Model Dev., 11, 257–281. https://doi.org/10.5194/gmd-11-257-2018.

[3] IPCC. 2018. Global warming of 1.5°C. An IPCC Special Report. [V. Masson-Delmotte, et al. (eds.)]. World Meteorological Organization, Geneva, Switzerland, 616 pp.

[4] ESRI. 2020. Docs. (access 08.02.2024, https://desktop.arcgis.com/en/documentation/).

[5] Stříž, M. 2008. Popis metod CLIDATA-GIS. (access 08.02.2024, http://www.infomet.cz/fil/1295510217.pdf).

Global variations of total electron content during the ionospheric storm on November 5, 2023

L. F. Chernogor, M. Yu. Tkachenko

V.N. Karazin Kharkiv National University, Kharkiv, Ukraine

A detailed study of the variations in Total Electron Content (TEC) in the ionosphere during geospace storms is significant both from a scientific and practical perspective. Ionospheric disturbances caused by geospace storms affect the propagation of radio waves, which is critically important for the reliable operation of systems such as radio communication, radar, radio astronomy, remote sensing, and navigation systems like GPS, BeiDou, and Galileo. Random variations in TEC can cause fading and scintillation of signals, hence their magnitude and the causes of these variations are important for improving the accuracy and reliability of various technological systems. Understanding TEC variations helps better predict the state of space weather, which is crucial for protecting space and terrestrial infrastructure from potentially harmful effects of geospace

storms. Geospace storms caused by solar activity and their impact on the Earth-atmosphere-ionosphere-magnetosphere system can damage or destroy onboard satellite electronics, affect aviation safety, and terrestrial technological systems. Studying the temporal variations of TEC also contributes to a deeper scientific understanding of the physical processes occurring under the influence of solar activity, which is important for the development of fundamental scientific theories.

The aim of the presentation is to present the results of the study of ionospheric effects during the geospace storm that occurred on November 5, 2023. The study of the temporal variations of TEC was conducted by analyzing global ionospheric maps with different time resolutions, created using the transionospheric sounding method with use of an international network of GNSS receiver stations. Data made publicly available by the Center for Orbit Determination in Europe (CODE, http://www.aiub.unibe.ch/download/CODE/) and The Crustal Dynamic Data Information System (CDDIS, https://cddis.nasa.gov/archive/gnss/products/ionex/) were utilized. Global ionospheric maps provided by the Technical University of Catalonia (UPC-IonSAT) with a 15-minute resolution and those from CODE with a one-hour resolution were also used.

We analyzed the state of space weather from November 2 to 8, 2023, including the main characteristics of the solar wind, interplanetary magnetic field, and geomagnetic field. The state of the ionosphere was analyzed on the eve of the magnetic storm (November 3), during the initial phase (November 4), the main phase (November 5), and the first day of its recovery phase (November 6). A positive ionospheric storm was observed, manifested by an increase in TEC values at all latitudes with peaks in the region of the equatorial ionospheric anomaly and the formation of troughs along the magnetic equator after sudden storm commencement at 16:00 on November 4, as well as at 08:00 and 13:00 on November 5. Distributions of absolute TEC values were constructed and analyzed, as well as their average values and medians for each interval. Global Electron Content (GEC) values were calculated and analyzed. An increase of 0.05-0.17 GECU in GEC values was detected, reaching a maximum of 2.23 GECU immediately after the first sudden storm commencement and a decrease to 1.65 GECU with the beginning of the recovery phase of the magnetic storm. At the same time, significant increases in GEC values were recorded after 08:00 on November 6, reaching peak values of 2.07 and 2.11 GECU at 20:00 and 22:00 respectively. Similar increases were observed for TEC values during the same period in the region of the equatorial ionospheric

anomaly with peaks on either side of the magnetic equator and a trough along the magnetic equator.

Variations in the ionospheric parameters during the maximum phase of the 25th cycle of solar activity

L.Ya. Emelyanov

Institute of Ionosphere, Kharkiv, Ukraine

The results of observations of the critical frequency (f_oF2), ionospheric F2 peak electron density (N_mF2) and peak height (h_mF2) of the ionosphere over Kharkiv (Ukraine, 49.6°N, 36.3°E) during the maximum phase of the 25th cycle of solar activity (2023) are presented. These data were obtained using the VISRC-2t ionosonde of the Institute of Ionosphere. Temporal variations of these ionospheric parameters were analyzed under conditions of low geomagnetic activity for typical geophysical periods (spring and autumn equinoxes, summer and winter solstices).

Diurnal variations in ionospheric parameters were mostly close to each other over three and more adjacent days for each season. The N_mF2 values averaged over three days reached $14.7\cdot10^{11}$, $5.6\cdot10^{11}$, $9.6\cdot10^{11}$, and $15.0\cdot10^{11}$ m^{-3} in the daytime and decreased at night to $2.3\cdot10^{11}$, $3.8\cdot10^{11}$, $2.6\cdot10^{11}$, and $1.4\cdot10^{11}$ m^{-3} in spring, summer, autumn, and winter, respectively. The difference in variations for different seasons is explained by different levels of solar activity, characterized by the $F_{10.7}$ index, the position of the Sun relative to the measurement site, and other geophysical factors. Significant differences between summer and winter variations are caused, in particular, by the presence of solar illumination of the ionosphere at the height of maximum ionization throughout the day in summer and the winter anomaly.

For all seasons, a comparative analysis of variations in N_mF2 and h_mF2 of the Kharkiv ionosonde was carried out with variations obtained using stations located at close latitudes to the Kharkiv ionosonde in the eastern and western hemispheres (https://giro.uml.edu/didbase/): Pruhonice (Czech Republic, 50.0°N, 14.6°E), Durbes (Belgium, 50.1°N, 4.6°E), Millstone Hill (USA, 42.6°N, 288.5°E). For comparison, temporal variations of N_mF2 and h_mF2 are presented as a function of local time (LT). The Pruhonice data turned out to be the closest to the Kharkiv data. The variations at Millstone Hill have the greatest difference, which indicates longitudinal effects in the

ionosphere associated with the mismatch of geographic and geomagnetic poles. The h_mF2 variations for all stations under consideration are quite similar, with the exception of some short periods of time. Values of h_mF2 in Millstone Hill are smaller at night in spring and autumn and larger during the day in autumn compared to those in Kharkiv, Pruhonice, and Durbes.

A comparative analysis of N_mF2 and h_mF2 diurnal variations of the mid-latitude ionosphere over Kharkiv with the same variations calculated using various options of the International Reference Ionosphere (IRI) model (https://irimodel.org/) and the ionospheric electron density model (NeQuick2) (https://t-ict4d.ictp.it/nequick2) was also carried out. For the IRI-2016 model, data were considered using three h_mF2 models and two maps for N_mF2. Both options of the IRI-2016 model and the NeQuick2 model give underestimated N_mF2 values for the spring equinox and summer solstice (except for 22 June) and overestimated values for the autumn equinox. The N_mF2 variations obtained from the IRI-2016 model are in good agreement with the experimental winter solstice data, and the NeQuick2 model significantly overestimates N_mF2 values.

The results of comparison of h_mF2 variations are as follows. The closest model to the Kharkiv results is the IRI-2016 (AMTB-2013) model. The IRI-2016 (CCIR-M2000) and IRI-2016 (Shubin) models describe h_mF2 variations somewhat worse. Autumn and winter daytime variations and summer nighttime variations are best described by the IRI-2016 model (Shubin). The results of calculating daily h_mF2 values using the NeQuick2 model for all seasons are the most distant from h_mF2 values in Kharkiv.

Changes in ion concentration and electric field near the Earth's surface

B. Hovorukha, L. Kozak, M. Solomakha

Taras Shevchenko National University of Kyiv, Kyiv, Ukraine

One of the most important aspects of experimental studies of atmospheric electricity is the measurement of electrical characteristics near the Earth's surface. The interpretation of experimental studies of atmospheric electricity is related to the selection of global changes in the electric field against the background of its local variations. The global atmospheric electric circuit determines the balance of electric currents in the atmosphere, the conditions for maintaining the electric field, as well as the structure of electric fields and currents. The data of long-term observations indicate the existence of an electric field with an intensity of the order and an electric

current with a density of the order in good weather conditions, that is, in the absence of clouds, winds, pollution, precipitation, etc. in this area. One of the first models of the global atmospheric electric field is the spherical capacitor model (Wilson model). In this model, it is assumed that the charging current occurs in all regions of the atmosphere that are occupied by thunderclouds. At the same time, dynamic equilibrium is performed in the atmosphere - the total charging current is equal to value of the total discharge current. Magnetohydrodynamic equations were used to model changes in the concentration of charged particles in the Earth's atmosphere and the electric field strength. At the same time, it is assumed that the spatio-temporal distribution of ion concentration in the surface layer is determined only by electrical forces. In the course of the research, the thickness of the electrode layer was determined and how it is affected by the mobility of various types of ions and the intensity of ion formation.

Relationship between Arctic sudden stratospheric warmings and total ozone variations over Europe

A.V. Grytsai[1], G.P. Milinevsky[2], R. Yu[2], O.M. Evtushevsky[1]

[1]Taras Shevchenko National University of Kyiv, Kyiv, Ukraine
[2]College of Physics, International Center of Future Science, Jilin University, Changchun, China

Sudden stratospheric warmings, a well-known phenomenon in the northern polar atmosphere with a mean frequency close to one event per two winter seasons, have been the focus of our research. These events sharply change the state of the stratospheric polar vortex and the distribution of various atmospheric parameters. In particular, stratospheric temperature increases by tens of degrees and intensive mixing of polar and mid-latitude air is observed. These processes influence total ozone values both in the polar and mid-latitude regions. While it is natural to expect total ozone increase in the high latitudes, the parameters of the phenomenon require further study. The corresponding variations in the moderate latitudes (in particular, over Ukraine) are not so evident, making our research a novel and intriguing contribution to the field.

The analysis of total ozone variations over several European stations with different latitudes (Kyiv-Goloseyev, Kaunas, Helsinki, Kiruna, Ny-Ålesund) has been conducted with utmost precision. Data for the North Pole have been included in the consideration to cover the highest latitudes. The

data of Multi-Sensor Reanalysis from 1979, which is based on observations of different origins (ground-based, ozonesonde, satellite), have been meticulously processed. This reanalysis provides appropriate data at the global scale. The climatology at all the stations is similar and typical for Europe with a spring maximum in February–April and an autumn minimum in October–November. We have utilized the method of superposing epochs (known also as composite analysis) to separate out variations connected with sudden stratospheric warmings, ensuring the accuracy and reliability of our results.

Our work shows relatively simple pattern in the high latitudes (Kiruna, Ny-Ålesund, North Pole) where total ozone increases after the date of warming by tens of Dobson Units (even by almost 100 Dobson Units in average) and exceeds climatological values during the several next weeks. These changes are a result of the penetrating of the mid-latitude air mass inside the stratospheric polar vortex region. Although the ozone hole does not usually appear in the Arctic, ozone values within the polar vortex are lower than in the middle latitudes. On the contrary, mid-latitude stations including Kyiv-Goloseyev have demonstrated total ozone decrease during one or two weeks after the warming. This feature is associated with a shift of the remnant of the stratospheric polar vortex from the polar region to the European longitudes. Seasonal properties of the warmings are also discussed.

Geomagnetic effect of the October 25, 2022 partial solar eclipse in the Euro-Asian region

L. F. Chernogor, M. Yu. Holub

V.N. Karazin Kharkiv National University, Kharkiv, Ukraine

A solar eclipse (SE) can cause disturbances in all subsystems of the Earth – atmosphere – ionosphere – magnetosphere system, including the geomagnetic field. The Earth's magnetic field is quite sensitive to disturbances of various physical nature and, especially, to disturbances on the Sun. In order to distinguish the response of the geomagnetic field to the SE, it is necessary to discard other possible sources. A careful analysis of space weather will come in handy. Against the background of the magnetic storm, which began on October 22, 2022 and lasted until the end of the day of October 24, 2022, it is difficult to select reference days. The day of October 27, 2022 was also disturbed ($K_{p\,\max}$ = 3, D_{st} from –20 nT to +20

nT). The quietest day was October 26, 2022. The day of October 21, 2022 was less quiet. These were the days chosen as reference days.

The effects of each SE have their own features. The feature of this eclipse was that it was observed against the background of the magnetic storm recovery phase, which means it could be masked by the storm. Distinguishing the effects of an eclipse against this background is an urgent and not trivial task.

The purpose of this report is to describe the results of observations of the geomagnetic effect caused by the SE in the Euro-Asian region. The partial SE of Saros 124 was observed on October 25, 2022 in Europe, the Middle East, Central Asia, western Siberia, and northwestern Africa. The SE started at 08:58:20 UT in Iceland in an area with geographic coordinates of 66°28′N, 18°57′W. The SE ended at 13:02:16 UT in the Arabian Sea area with coordinates of 17°35′N, 66°31′E. The largest magnitude of the SE reached 0.8623. It was observed in the area with coordinates of 61°36′N, 77°24′E. The SE magnitude at the stations varied from 0.210 to 0.838, and the relative obscuration area of the solar disk from 11 to 79%.

Using data obtained at 15 stations of the INTERMAGNET network, the temporal variations of all components of the geomagnetic field were analyzed. The amplitude resolution was 0.1 nT, and the time resolution was 1 min. Before analyzing variations in the geomagnetic field level, the constant component was removed. The trend of these geomagnetic field components was additionally calculated over an interval of 60 min to detect the aperiodic effect.

It was established that the SE was accompanied by a disturbance in the level of the *X*-, *Y*- and *Z*-components. The largest disturbances occurred in the *X*-component (south–north). A strong tendency towards increasing the disturbance magnitude in the *X*-component level with increasing the area of solar disk obscuration was observed. Calculation of the disturbance magnitude in the *X*-component level under the SE influence has been performed. It was believed that the main mechanism for generating the magnetic effect was a disturbance in the system of ionospheric currents at the dynamo region heights. The results of observations and calculations are in good agreement with each other. In addition to the persistent aperiodic effect lasting about 100–180 min, an increase in the range of fluctuations in the geomagnetic field level throughout the SE was observed. This may indicate the generation of quasi-periodic geomagnetic field disturbances in the range of atmospheric gravity waves.

The study was partially supported by State Budget grants provided by the Ministry of Education and Science (registration no. 0122U001476 and 0124U000478).

Fractal properties of the processes in the Sun–Earth system

L.F. Chernogor[1], O.V. Lazorenko[1], A.A. Onishchenko[2]

[1]V.N. Karazin Kharkiv National University, Kharkiv, Ukraine
[2]Kharkiv National University of Radio Electronics, Kharkiv, Ukraine

According to the non-linear and the system paradigms, many processes generated in the Sun – Earth system being an open, non-linear, dynamical system, under influence of a powerful source of energy release are appeared to be short-time, ultra-wideband, non-linear and fractal. This fact can be explained by existence of very complex and manifold interactions which observed between different subsystems. Many processes caused in the Sun – Earth system by the non-stationary powerful sources of energy release have significant fractal properties. Therefore, the investigations of such properties seem to be actual, interesting and useful. The purpose of this work is to present real proofs of the fractal properties existence for the processes generated in the Sun – Earth system under influence of a powerful source of energy release.

Some traditional and new numerical characteristics, which describe well the fractal properties of the processes in the Sun – Earth system and were obtained by application of both the mono-fractal and the multifractal analyses, are briefly considered. Let's consider them in detail. Many processes in the Sun were occurred to be fractal and multifractal. First, in 1969, B. Mandelbrot and J. Wallis found that in *the Wolf number time series* in both period bands from 3 to 30 months and from 30 to 100 years, the fractal dimension was appeared to be $D \approx 1.1$. Subsequently, it was established that the time series of Wolf numbers can be considered as a fractal process, which is well described by the generalized Brownian motion model with the fractal dimension values in bounds $D = 1.1 \div 1.3$. The fractal dimension D_A of the phase trajectory attractor of the system, with is principally able to create such time series, was found to be in bounds $D_A = 2.8 \div 0.1$. Second, *the time series of global Solar radiation* detected in 1990 – 2004 was shown to be anti-persistent with the fractal dimension value $D = 1.93$.

Different fractal properties were found in the interplanetary and Earth's magnetic fields. One hand, according the experimental data obtained by the "Voyager-2", *the time fluctuations of the interplanetary magnetic field* have the self-similarity properties for periods ranging from 20 s to 3×10^5 s and have the fractal dimension value D = 5/3. Other hand, *the D_{st} index time*

series was found to be a multi-fractal process, which is well described by the multi-fractal Brownian motion model. There were some attempts to apply these fractal and multifractal properties of the D_{st} index time series for forecasting of the magnetic storm appearance.

As an example of *the fractals in the ionosphere*, the results of the investigations of the multifractal structure of fragmented fractional-scale ionospheric turbulence during the specialized experiments from radio transmission of the mid-latitude ionosphere by signals from Earth's orbital satellites performed in 2005 – 2006 can be considered.

Following the famous geophysicist H. Takayasu, we can repeat: "*The earthquakes* have so many different fractal properties, that they can be classified as the most interesting fractal phenomena". Different fractal properties were successfully discovered, for example, in the time distribution of aftershocks ("Omory's Law"), in the relationship between the number of earthquakes and their magnitude or total energy ("Guttenberg – Richter Law"), in the spatial distribution of earthquake sources, in the spatial structure of the seismogenic geotectonic faults, in the process of the appearance of earthquakes in time, in the seismoelectric signals, in the acoustic radiation of the ultrasonic range, in the variations of the geomagnetic field in the ultra-high frequency range, in the single scaling law for earthquakes and in many others.

Statistical characteristics of seismic waves and tsunami generated by the 2022 Hunga Tonga volcanic eruption

L.F. Chernogor[1], Y. Luo[1,2]

[1]V.N. Karazin Kharkiv National University, Kharkiv, Ukraine
[2]Ghent University, Ghent, Belgium

On January 15, 2022, the Hunga-Tonga-Hunga-Haapai volcano in the Kingdom of Tonga unleashed a catastrophic explosive eruption, marking a significant event in geological history. This eruption, documented at geographical coordinates 20°54′S, 175°38′W, comprised five powerful explosions, with the most significant occurring at 04:15 UT and accompanied by a magnitude Ms ≈ 5.8 earthquake. The seismic source's energy was estimated between 6.5–23 TJ and 19–69 TJ in various reports, while the associated air wave's energy ranged from 16.7–75.3 TJ to 2 ± 0.8 PJ. Classified as a super volcano, with a total energy release not surpassing 17.6 ± 2.7 Mt TNT or 73.6 ± 11.3 TJ and an eruption's thermal energy

approximately 3.9×10^{18} J or 932 Mt TNT, the eruption instigated significant disruptions across various Earth subsystems, including the lithosphere, oceans, atmosphere, ionosphere, and magnetosphere. The intricate physical effects have been extensively discussed in numerous studies, with seismic and tsunamigenic effects thoroughly documented in seismic and tsunami-related literature. This paper focuses on the statistical characteristics of seismic waves and tsunamis generated by the eruption, aiming to present statistical assessments concerning the mechanical properties of Rayleigh waves, slow seismic waves, and tsunamis following the eruption.

Seismograms were collected from stations within the Global Seismographic Network (GSN) operated by the Incorporated Research Institutions for Seismology Consortium (IRIS) [https://www.usgs.gov/programs/earthquake-hazards/gsn-global-seismographic-network]. General Information concerning the tsunami is accessible through the database provided by FDSN (International Federation of Digital Seismograph Networks) [https://www.fdsn.org/networks/ detail/NZ/] and GEONET [https://tilde.geonet.org.nz/ui/data-exploration/Dart], which is specific to New Zealand.

Our statistical analysis primarily involved the generation of correlation fields (scatter diagrams), the formulation of regression equations, and the calculation of statistical parameters related to key parameters (Rayleigh wave, Lamb air wave, long waves in water, and tsunami) resulting from the 2022 Tonga volcano's explosion. The statistical analysis unveils several crucial insights, including: 1) Both the amplitude and speed of mechanical vibrations on the Earth's surface display a power-law decrease with distance, indicating the attenuation of seismic energy over spatial extents. 2) For tsunamis, there is a noticeable attenuation of wave energy with distance, with the height of the tsunami adequately captured by a decreasing power function, and its arrival time effectively represented by linear functions. 3) The arrival time of Rayleigh waves follows a linear function, suggesting consistent propagation characteristics with an average speed of 3.77 km s^{-1}, while the independence of Rayleigh wave speed from distance is justified, estimated at 3.76 ± 0.26 km/s. 4) Seismic waves originating from the atmosphere exhibited a velocity of 306 ± 9 m/s, closely aligned with the Lamb wave speed of 313 m s^{-1}. 5) The seismic wave of hydrodynamic origin displayed a velocity of approximately 236 ± 28 m s^{-1}, while the tsunami itself exhibited a velocity in the vicinity of 256 ± 29 m s^{-1}. These findings contribute to our understanding of the mechanical dynamics associated with volcanic eruptions and their impact on seismic and tsunami phenomena.

Work of L.F. Chernogor was supported by the Ukraine state research project #0122U001476 and #0124U000478, and work of Y. Luo was supported by the Special Research Fund of Ghent University of Belgium (project #BOF22/CDV/061).

Features of ionospheric disturbances caused by the solar eclipse on April 20, 2023

L.F. Chernogor, Yu.B. Mylovanov

V.N. Karazin Kharkiv National University, Kharkiv, Ukraine

The purpose of the work is to describe the features of the ionospheric effects of the hybrid solar eclipse (SE) on April 20, 2023, observed in the southern and eastern parts of the Indian Ocean. The eclipse began in the subpolar zone of Antarctica and then moved towards the equator. We have studied temporal variations in total electron content (TEC), which was measured using a global satellite navigation system. For this purpose, 36 ground-based stations and a number of satellites were used (G01, G03, G04, G06, G07, G08, G09, G14, G16, G17, G18, G19, G21, G22, G26, G27, G30, G31). The space weather state was favorable for studying the SE effects in the ionosphere.

The hybrid (in this case the total eclipse was replaced by an annular) SE began at 01:34:23 UT northwest of the Kerguelen archipelago (France), and ended at 06:59:14 UT east of the Marshall Islands in the Pacific Ocean. From 02:00 UT to 05:00 UT the lunar shadow moved northeast until it crossed the equator and further to the east. The eclipse magnitude reached a maximum value of 1.0132 at 04:16:37 UT in East Timor. With the further movement of the lunar shadow with the arrival of the morning solar terminator and an increase in the intensity of solar radiation, a picture of the eclipse became more complicated. Despite the influence of diurnal TEC variations, we were able to confidently detect the ionospheric effects of the SE.

A feature of the SE was the passage of the lunar shadow in the subpolar, mid-latitude and equatorial regions. The distribution of observation stations near the trajectory of the lunar shadow made it possible to estimate the TEC at the maximum overlap of the solar disk by the Moon. In the southern Indian Ocean, the number of observation stations was insufficient, and they

were located mainly on the northern coast of Antarctica. On the contrary, there were quite a lot of stations on the western and northern coasts of Australia and on the islands of Indonesia. This made it possible to clarify the ionospheric behavior under solar eclipse conditions in the time period from 03:00 UT to 05:00 UT.

A new technique for estimating the expected TEC values in the eclipse time interval has been applied. For this purpose, TEC values on reference days and the global ionospheric map on the day of the eclipse were used. This made it possible to substantiate the method for determining the TEC values expected in the absence of an eclipse and to significantly reduce the influence of the human factor on the assessment of the TEC deficit.

As is known, a decrease in TEC may not occur immediately after the onset of an eclipse, and the duration of an eclipse and the duration of the ionospheric response may not coincide. The decrease in TEC was specified; it turned out to be directly proportional to the obscuration area of the solar disk and is approximately equal to 0.6 TECU for every 10% of the obscuration area. When this area reaches 90%, TEC decreases by 10–15 TECU.

The maximum value of the TEC deficit is generally achieved 20–30 min after the maximum magnitude of the eclipse and significantly depends on the position of the lunar shadow trajectory, measurement points in the *F*-region of the ionosphere and diurnal changes, including the movement of the solar terminator. The delay time of the ionospheric response to the maximum magnitude of the SE indicates the inertia of chemical processes in the *F*-region of the ionosphere.

Measuring the TEC deficit in the morning, evening and noon with an eclipse magnitude from 0.2 to 0.9, taking into account more precise technique for estimating expected values, made it possible to more accurately assess the relationship between the eclipse magnitude (obscuration area of the solar disk) with the subsequent TEC deficit. The magnitude of the TEC deficit significantly depended on the SE magnitude, time of day, and latitude. These were the main features of this SE.

This work has been partially supported by the Ministry of Education of Ukraine (grants No. 0122U001476 and No. 0124U000478).

Main features of the geomagnetic effect of the October 14, 2023 annular solar eclipse in the America

L.F. Chernogor, V.T. Rozumenko

V.N. Karazin Kharkiv National University, Kharkiv, Ukraine

The main features of the October 14, 2023 solar eclipse include its annularity, its occurrence from local dawn to local dusk, its magnitude variation from 0.30 to 0.86, and the longest ever-observed path across the mainland of the Americas, covering latitudes from ~65°N to 12°S. The analysis was made possible due to the data on temporal variations in the northward, *X*, eastward, *Y*, and vertical, *Z*, components of the geomagnetic field collected at thirteen International Real-time Magnetic Observatory Network magnetometer stations (https://imag-data.bgs.ac.uk/GIN_V1/GINForms2). A solar eclipse is a convenient solar-terrestrial phenomenon of opportunity for studying coupling in the solar-terrestrial system comprised of the sun, interplanetary medium, magnetosphere, ionosphere, atmosphere, and solid earth. In the course of a solar eclipse, a number of parameters become disturbed in all subsystems and geophysical fields, and in particular, in the geomagnetic field. Generally, the geomagnetic effect of solar eclipses has been studied for over 120 years. Despite the long history of geomagnetic effect from solar eclipses studies, even the question of whether the effect exists or does not occur, still remains more or less open to date. The following data processing algorithm was employed. First, DC components, different for different stations, are subtracted from the raw data, and the dependences $X(t)$, $Y(t)$, and $Z(t)$ are formed. Then, the 60-min running averages are used to form temporal variations in the $\overline{X}(t)$, $\overline{Y}(t)$, and $\overline{Z}(t)$ trends. In addition, the differences between $X(t)$ and $\overline{X}(t)$, $Y(t)$ and $\overline{Y}(t)$, as well as between $Z(t)$ and $\overline{Z}(t)$ are calculated. The dependences $\overline{X}(t)$, $\overline{Y}(t)$, and $\overline{Z}(t)$ are used for finding the non-sinusoidal solar effect, and the differences are used for revealing possible quasi-sinusoidal perturbations in the geomagnetic field.

Analysis of temporal variations in all components of the geomagnetic field recorded at thirteen magnetometer stations at more than ~8000 km distance apart on the day the solar eclipse occurred and during magnetically quiet times showed the following: (i) The solar eclipse acted to produce a decrease of up to 10–20 nT in the magnitude of the strength of all

geomagnetic field components. The *X*-component experienced the greatest disturbance, while the *Z*-component was disturbed the least. The duration of the perturbation was observed to be ~120–240 min, while the onset of the decrease in the strength was delayed by 80–100 min relative to the solar eclipse first contact. (ii) In addition to the non-sinusoidal perturbations in the geomagnetic field, quasi-sinusoidal variations of up to 5–15 nT were recorded, although usually they did not exceed 5–6 nT. The oscillation period showed variations within 10–80 min, but it was most often found in the 15–40-min range. The time delay of the appearance of quasi-sinusoidal perturbations varied from 30 to 150 min, but most often from 80 to 90 min. The quasi-sinusoidal perturbations persisted for 180–240 min. (iii) A tendency was shown for the magnitude of the non-sinusoidal and quasi-sinusoidal perturbations to increase as the solar eclipse magnitude increased. (iv) The magnitude of the geomagnetic effect of the solar eclipse is significantly dependent on the geographic coordinates of the magnetometer station, local time, the state of the ionosphere and ionospheric current system. (v) The electron density depletion was estimated to be ~ 0.10 to ~ 0.40–0.60 when the eclipse obscuration A_{max} varied from 19% to 82%. (vi) The movement of the lunar shadow was accompanied by the generation and propagation of atmospheric gravity waves with ~10–80-min periods and by electron density perturbations with relative amplitudes of the order of 0.01–0.03. (vii) The estimates made on the assumption that the magnetic effect of the solar eclipse is due to the ionospheric current disruption show good agreement with the observations.

This work has been partially supported by the Ministry of Education of Ukraine (grants No. 0122U001476 and No. 0124U000478).

The primary outcomes of the two-year air pollution monitoring conducted during military actions in Ukraine

M. Savenets, L. Nadtochii, T. Kozlenko, K. Komisar, A. Umanets, N. Zhemera

Ukrainian Hydrometeorological Institute, Kyiv, Ukraine

After a two-year period of the full-scale russian invasion of Ukraine, continuous emissions of air pollutants, redistribution of emission sources, and damages to industrial facilities significantly influenced air quality. The most challenging issues arise with monitoring data availability. While remote sensing was often affected by cloudiness and depended on spatial resolution, ground-level observations were sparse, with frequent gaps and

the impossibility of being conducted near the frontline. After spending two years collecting air quality data from different systems of basing, quality control, and post-processing at the Ukrainian Hydrometeorological Institute (UHMI), we step by step outlined the main consequences of russian military aggression on air pollution in Ukraine at different temporal scales. The study was carried out using satellite measurements from TROPOMI and MODIS instruments, combined with ground-level air pollution observations at about 100 monitoring sites from the databases of the Central Geophysical Observatory (CGO), named after Boris Sreznevskyi, Kyiv, Ukraine. Depending on the temporal and spatial scales, the war consequences for specific chemical species vary a lot. Satellite data at a coarser spatial resolution revealed a decrease in nitrogen dioxide (NO_2) and carbon monoxide (CO) as a result of industry damage. On a local scale, we observed short-term air pollution, especially immediately after missile attacks. Some extreme elevated pollutants' content showed a 500–10000% spike in concentrations in comparison to values before the attack. Considering fuel use redistribution and damage to energy objects, we estimated burning efficiency using the NO_2/CO ratio. Its drop in Ukrainian cities by 11–46% indirectly proved the increase in solid or "dirty" fuel use and less gas consumption. Changes in aerosol parameters (aerosol optical depth (AOD), Angstrom exponent, and aerosol mass concentration) are mostly detectable using remote sensing over wildfires near the frontline and during fires on oil depots.

The profile of ozone measured by microwave radiometer RSO3CO in winter 2023/2024 over Changchun, Northeast China

Y. Shi[1], G. Milinevsky[1,2]

[1]Jilin University, International Center of Future Science, Changchun, China
[1]Main Astronomical Observatory of NAS of Ukraine, Kyiv, Ukraine

In recent years, microwave remote-sensing technology has developed rapidly in the field of atmospheric science. As a passive remote sensing device, ground-based microwave radiometry (MWR) does not actively emit electromagnetic waves but only passively receives radiation in the direction of the target, which makes it an excellent atmospheric remote sensing device. Its advantages are low power consumption, high spatial resolution, and long observation time, which assist in achieving long-term monitoring of the middle atmosphere. Worldwide, a number of radiometers have been

developed to observe ozone and water vapor, and various microwave observation techniques, radiometer calibration methods, and data processing techniques to obtain molecular volume mixing ratio profiles have been used. This study discussed long-term monitoring of the ozone profile in the winter of 2023/2024 using a microwave radiometer RSO3CO located in Changchun, northeastern China, with a focus on the distribution of ozone (O_3) in the upper and middle stratosphere. The ground-based remote sensing technology is used to continuously monitor the frequency of O_3 rotation transition (615→606) at 110.836 GHz. The RSO3CO radiometer can provide a vertical profile of ozone in the atmosphere, covering an altitude range of 25–90 km. The whole process of the data retrieval from the MWR ozone measurements in the atmosphere is multistage and complicated, including several program packages such as the ARTS forward model and the Qpack program, which run under the Ubuntu operating system. We calculated it using volume mixing ratio (VMR) and concentration units and compared the results with meteorological satellite data. The research results indicate that the maximum volume mixing ratio of ozone is located in the stratosphere, whereas the highest concentrations appear at lower altitudes. In addition, we studied the ozone content, which showed an increasing trend in mid-February, which may be related to the sudden stratospheric warming event in the polar stratosphere.

Change in the electrical characteristics of the atmosphere in the presence of aerosols

X. Sun[1], M. Solomakha[2], L. Kozak[2], G. Milinevsky[3], B. Hovorukha[2]

[1]College of Electronic Science and Engineering, International Center of Future Science, Jilin University, Changchun China
[2]Taras Shevchenko National University of Kyiv, Kyiv, Ukraine
[3]College of Physics, International Center of Future Science, Jilin University, Changchun, China

The main characteristics of the electrical state of the atmosphere (electric field strength, electric charge density, electric current density, electric field potential, and electrical conductivity of the atmosphere) are local and related quantities. The electrical conductivity of the atmosphere is determined by the chemical nature of the molecules that make up the atmosphere, the diffusion coefficient, and their motion. According to modern concepts, the main contribution to the electrical conductivity of the

lower atmosphere is made by light ions that are generated under the influence of radioactive exposure from the Earth's surface, radioactive impurities and cosmic rays. The presence of aerosol particles leads to changes in the concentration of positive and negative light ions. The analysis of the characteristics of different types of aerosols and experimental data showed that particles with a size of 0.01 – 0.2 μm affect the value of atmospheric electricity, and the concentration of these particles depends on the area. Numerical modeling of the effect of aerosols on the change in the electrical characteristics of the surface layer was carried out for concentrations of aerosol particles in the range of 10^7 – 10^9 m^{-3}. It was shown that at $N<10^8$ m^{-3} the aerosol practically does not affect the distribution of ion concentrations in the ground layer, and an increase in concentrations to values of the order of 5 10^8 – 10^9 m^{-3} leads to a decrease in the thickness of the electrode layer.

Ground-based microwave radiometer with a cooling front-end for ozone and carbon monoxide monitoring in the stratosphere and mesosphere

X. Sun[1,2], L. Wang[1,2], Y. Shi[1,2], G. Milinevsky[1], X. Wang[2], O. Pylypenko[1]

[1]College of Physics, International Center of Future Science, Jilin University, Changchun, China
[2]College of Electronic Science and Engineering, International Center of Future Science, Jilin University, Changchun, China

Microwave radiometers have great potential in remote sensing techniques for measuring vertical profiles of stratospheric and mesosphere gases. Because microwave signals can penetrate clouds, light rain, and fog, microwave radiometers are less affected by weather changes and have high stability. The ground-based microwave radiometer is the only measurement method to monitor the middle atmosphere day and night and all weather. The emission frequency of ozone molecules in the atmosphere is 110.836 GHz, and CO is 115.271 GHz. Microwave technology is also used to measure mesospheric wind speed, which is a research hotspot. In this report we describe a new type of microwave radiometer, a dual-frequency receiver with a cooled front-end, which can measure CO/O_3 molecules simultaneously and allows atmospheric dynamics monitoring. The design uses the more compact and economical Peltier cooling technology. In the

design, the cold load and the radiofrequency receiver are placed together in a metallic aluminum housing and cooled by two Peltier elements. To prevent the effects of water vapor condensation at low temperatures, the air inside the metal chamber is drained and filled with dry nitrogen. In order to ensure the accuracy of measurement, it is necessary to develop high-performance cold loads with high emissivity and low temperature gradients. The conical array structure and conical cavity structure of the spaceborne radiometer are not used in this design. But designing a wedge cooling load can further improve the accuracy of microwave radiometer measurement. The layout of the new radiometer, expected parameters and novel design decisions are discussed.

The geomagnetic effect of the Kyiv meteoroid

L.F. Chernogor, N.M. Tilichenko

V.N. Karazin Kharkiv National University, Kharkiv, Ukraine

Theoretical and experimental research of the geomagnetic effect of space bodies remains an urgent task. This is especially true for meter-sized meteoroids, for which the existence of a magnetic effect remains in question. The space body entered the Earth's atmosphere over the Kyiv region, Ukraine, on April 19, 2023. We named it the Kyiv meteoroid. A cascade destruction of the body took place, accompanied by five thermal explosions of large fragments in the altitude range from 38 to 28 km. The coordinates of the most powerful explosion are as follows: 49.5°N, 29.9°E. The initial speed of the meteoroid was 29 km s^{-1}. According to our estimates, the total optical radiated energy of the meteoroid reached 25.2±2.5 GJ, the initial kinetic energy did not exceed 0.09±0.01 kt of TNT ≈ 375±35 GJ. With a body mass of 0.89±0.09 t, its volume was close to 0.25±0.025 m^3, and its size did not exceed 79±3 cm. The angle of inclination of the trajectory to the horizon was 32°.

The purpose of this work is to present the results of the analysis of time variations of the levels of the *X*-, *Y*- and *Z*-components of the geomagnetic field, registered by the INTERMAGNET network of magnetic stations on the day of the fall of the Kyiv meteoroid and on reference days. The analysis of time variations showed that the level of these components on the day of the explosion of the cosmic body and on the reference days differed significantly. The *X*-component level with a delay time of 6 min decreased

by 2–5 nT, which lasted about 60 min. It was established that the disturbance of the *X*-component level depended on the distance according to the law, which is typical for cylindrical waves propagating in a waveguide. The attenuation depth was close to 3850 km.

A quasi-periodic disturbance was observed with a delay time of 25 min and a duration of 25 min with a variable period within 4–12 min and an amplitude increasing from 0.3–0.4 to 1.2–1.5 nT. The first disturbance, which had a speed of about 300 m/s, could be caused by an explosive wave. The second perturbation is most likely related to the generation and oblique propagation at hundreds of meters per second of an atmospheric gravity wave. Within the ionosphere, the disturbance propagated at a speed of ~660 km/s with the help of magnetohydrodynamic waves. Temporal variations in the levels of *Y*- and *Z*-components on the day of the explosion, fluctuating for ~60 min, decreased by 5–10 nT. The mechanism of long-term disturbances of these components remains unknown. It is likely that it could be related to the diamagnetic effect. Thus, it is established that cosmic bodies of meter size are able to cause a recorded magnetic effect.

The study was partially supported by State Budget grant provided by the Ministry of Education and Science (registration no. 0122U001476).

Imaging polarimeter for the stratosphere aerosol study from the near-earth orbit at the wavelength 1.378 μm

I. Syniavskyi[1], V. Danylevsky[2], Yu. Ivanov[1], M. Sosonkin[1], Ye. Oberemok[2], Zh. Dlugach[1], G. Milinevsky[1,3]

[1] Main Astronomical Observatory of the National Academy of Sciences of Ukraine, Kyiv, Ukraine
[2] Taras Shevchenko National University of Kyiv, Kyiv, Ukraine
[3]College of Physics, International Center of Future Science, Jilin University, Changchun, China

The stratosphere is an important part of the Earth's atmosphere that has a significant influence on the Earth's climate as a planet. Stratospheric aerosol particles may also have an important role in climate formation despite their low concentration compared to the tropospheric aerosol. The aerosol particles content in the stratosphere can vary significantly mainly depending on volcanic activity and various powerful events such as dust storms and wildfire. Modern instruments for aerosol studying in the stratosphere still provide insufficient amount and accuracy of measurements. Therefore,

development of new effective techniques for measurements and the continuous monitoring of the aerosol in the stratosphere is the relevant field of scientific research.

Some publications discuss a new technique for stratospheric aerosol observations from near-earth orbit using the water vapor spectral absorption band at 1.378 μm. The polarimetry is considered as a very effective technique for this research. We design multispectral imaging polarimeters MSIP for the Aerosol-UA project. The polarimeter for the short-wave infrared measurements with a spectral wavelength of 1.378 μm can be proposed for study of the stratospheric aerosol optical depth and particle properties. The full field of view of the polarimeter is 60°x60° with spatial resolution of 0.5°x0.5°. The polarimeter measures the first three Stokes parameters (*I, Q, U*) of the solar radiation scattered by the stratosphere over the dark surface because water vapor concentrated mainly in the troposphere absorbs the radiation at 1.378 μm. The special optical wedges are used in the polarimeter's optical system to divide the entrance optical beam and form four separate images of the field of view. The linear analyzer installed in each of the separate optical beams, and axes of the analyzers oriented with angles of 0°, 45°, 90°, 135°. Thereby three Stokes parameters are measured at the same time. Also, a radiometric channel of MSIP with four wavelengths of range 860 to 940 nm was added to determine water vapor content in the troposphere following MODIS procedure. The size and weight of the polarimeter are small and can be installed on the 12U microsatellite.

Suitability of this instrument for the stratosphere aerosol study was estimated using intensity of solar radiation at 1.375 μm scattered by the Earth atmosphere and measured with ENVISAT satellite. Also, the irradiance of the polarimeter on the near-earth orbit with altitude 700 km by scattered solar radiance was calculated using the stratosphere aerosol properties models. Aerosol particle size distribution was single-mode lognormal with modal radius and distribution width corresponding to the ones determined by different techniques, and particles refractive index corresponded to 75% H2SO4 water solution at the stratosphere temperature. The simulations were performed for the aerosol optical depth ranging from 10^{-4} to 10^{-1} over the dark surface. The polarimeter output signal at these circumstances was acceptable for registration and analysis.

[1] Kovilakam, M., Thomason, L. W., Ernest, N., et al., 2020: The global space-based stratospheric aerosol climatology (version 2.0): 1979–2018. Earth Syst. Sci. Data, 12, 2607–2634.

[2] Mishchenko, M. I., Dlugach, J. M., Lacis, A. A., et al., 2019: Retrieval of volcanic and man-made stratospheric aerosols from orbital polarimetric measurements. Opt. Express 27, A158–A170.

[3] Dlugach, J. M., Mishchenko, M. I., Veles, O. A., 2021: Applying orbital multi-angle photopolarimetric observations to study properties of aerosols in the Earth's atmosphere: Implications of measurements in the 1.378-μm spectral channel to retrieve microphysical characteristics and composition of stratospheric aerosols. J. Quant. Spectrosc. Radiat. Transf. 261, 107483–107502.

[4] Syniavskyi I., Oberemok Ye., Danylevsky V., et al., 2021: Aerosol-UA satellite mission for the polarimetric study of aerosols in the atmosphere. J. Quant. Spectrosc. Radiat. Transf. 267, 107601.

The impact of dust storms events on air quality in Changchun, China

X. Wei[1], Y. Yukhymchuk[2], G. Milinevsky[1,2], Y. Shi[1]

[1]College of Physics, International Center of Future Science, Jilin University, Changchun, China
[2]Main Astronomical Observatory of NAS of Ukraine, Kyiv, Ukraine

Particulate matter (PM) is an air pollutant that have negative effects to human health. Although China has been continuously improving air quality through governance in recent years, research has shown that air pollution caused by $PM_{2.5}$/PM_{10} still can be significant. Particulate matter may have origin from indoor and outdoor sources. The purpose of this study is to explore the impact of dust storms events on indoor and outdoor air quality in Changchun City. Changchun is located in Northeast China and is a city with a large number of residential buildings. In this study, we monitored and analyzed the concentrations of indoor and outdoor $PM_{2.5}$ and PM_{10} in a urban area of the city. We provided monitoring of indoor and outdoor concentrations of $PM_{2.5}$ and PM_{10} in the Changchun city from April 5th to October 31st, 2023 using two AirVisual devices and one Air Quality Monitor SDL607 installed in residential area of the city (43.83°N, 125.28°E), two monitors indoor in the living flat, and one outdoor in the same address. In this study, we evaluated $PM_{2.5}$ and PM_{10} concentrations with a different time interval. For analysis, we also used data on the temperature changes, precipitation, wind speed, and wind direction based on measurements at the weather station in Changchun (https://meteostat.net/, WMO 54161 weather station). According the measurements, in spring,

summer, and autumn, the air quality in Changchun city is mainly related to the wind direction. Especially in spring, the wind blowing from the west will bring a large amount of particles from the Gobi Desert in the west, causing dust storm events and increasing the concentration of $PM_{2.5}$ and PM_{10} in the air.

The impact of Tonga volcano eruption on the mid-latitude atmosphere by producing large amounts of water vapor

R. Yu[1], Y. Shi[1], G. Milinevsky[1,2]

[1]College of Physics, International Center of Future Science, Jilin University, Changchun, China
[2]Main Astronomical Observatory of NAS of Ukraine, Kyiv, Ukraine

On 15 January 2022, the large the intra-oceanic Hunga volcano (Hunga Tonga-Hunga Haapai) in the South Pacific Ocean exploded violently. The Hunga volcano is located at 20.553°S, 175.384°W, and locates about 65 kilometers north of the capital of the Kingdom of Tonga. The eruption, which began in the South Pacific, roiled nearly half the world. The volcanic eruption event has received widespread attention from the scientific community. Research shows that the catastrophic eruption triggered giant atmospheric waves. It will have an impact on the global climate for a long time, and even affect the atmospheric dynamics of the Northern Hemisphere. In this work, we use Aura MLS satellite data to retrieve the changes in the water vapor and ozone profiles in the atmosphere over the volcanic eruption region and over the mid-latitude region of northeast China during the 2021–2024 period: the year before the eruption and more than two years after. We use the RSO3CO data, a microwave radiometer located in Changchun City (43.85°N, 125.33°E) in northeast China, to search for the impact of volcano products on stratospheric ozone profiles measured by this microwave radiometer. The results show that on the 10th day after the eruption, water vapor in the volcano area suddenly increased and was gradually transported into the stratosphere over time. In addition, the troposphere and mesosphere in northeast China also exhibit a significant increase in the VMR water vapor by MSL data in the upper stratosphere and mesosphere since May 2023. Compared with the changes in water vapor, the change in ozone content over northeast China in connection to the post effect of the volcano eruption, according to our MWR measurements, is not

so obvious. The long-lasting impact of the Tonga volcanic eruption on the atmospheric environment in the Northern mid-latitudes is discussed.

Response of the troposphere to 27-day solar activity cycles

I.G. Zakharov, L.F. Chernogor

V.N. Karazin Kharkiv National University, Kharkiv, Ukraine

Studying the influence of solar activity on the troposphere is important for increasing the accuracy of weather forecasts and better understanding the interaction of atmospheric layers. These circumstances determine the relevance of our research. Research objectives are to identify 27-day solar-induced cycles in the troposphere and to investigate their main characteristics. The study was carried out for the decline phase of the 23rd 11-year solar cycle with high-amplitude and similar 27-day cycles. Longitudinal and latitudinal changes in sea level pressure, temperature and zonal wind in the troposphere and lower stratosphere, as well as tropopause height in the northern hemisphere, were considered. All atmospheric data are taken from the website https://psn.noaa.gov, solar data – from the website https://www-app3.gfz-potsdam.de.

It has been established that the longitudinal changes in all specified parameters have maximum amplitudes of 27-day oscillations over the continents (Europe and North America), which appear in antiphase to each other. As a consequence, their zonally averaged variations, which are usually considered in the scientific literature, are several times smaller.

Latitudinal changes in specified indicators are characterized by association to the elements of the global circulation in the troposphere (Hadley, Ferrell and polar atmosphere cells), and in the lower stratosphere to the features of the Brewer-Dobson circulation. Pressure and zonal wind have maximum amplitudes of 27-day oscillations inside these cells with a change in the sign of anomaly at the cell boundaries. Tropospheric temperature changes are maximum at the cell boundaries. There is also a shift in the position of the jet streams by more than 1° in latitude. At high latitudes, there is a gradual time shift in the phase of zonal wind oscillations (up to ~ 10 days) during the transition from the stratosphere to the troposphere, which can be considered as a manifestation of the downward influence of the stratosphere on the troposphere.

The largest amplitudes of solar-induced anomalies occur in northern part of the Ferrell cell and the southern part of the polar atmosphere cell (50–

70°N latitudes) and reach 5.3K for surface temperature, 3.5 K for temperature of the lower stratosphere, 12 hPa for sea level pressure, 7 m s^{-1} for zonal wind with a maximum in the upper troposphere, as well as 1.2 km for tropopause height. At low latitudes, 27-day variations in all indicators are minimal.

The main driver of solar forcing is the 27-day variation in solar UV radiation, leading to cyclical changes in temperature and wind field in the stratosphere. Changes in the troposphere are realized through two-way dynamic interaction of the troposphere and stratosphere, similar to the stratospheric-tropospheric interaction during sudden stratospheric warmings, but with a smaller amplitude in the stratosphere. Solar effects are recorded in all seasons, the maximum effect is observed in winter. The presence of a reliable response in summer, when upward propagation of planetary-scale Rossby waves is hindered, indicates the important role of synoptic-scale and internal gravity waves, which can provide the upward propagation of waves through nonlinear wave–wave interaction.

This work has been partially supported by the Ministry of Education of Ukraine (grants No.0122U001476 and No.0124U000478).

Characteristics of large-scale traveling ionospheric disturbances over Europe, North America and South Africa during the geospace storm on 27 -28 February 2023

S.V. Panasenko[1], V.V. Skipa[2], M.O. Reznychenko[1,3]

[1]Institute of ionosphere, Kharkiv, Ukraine;
[2]Institute of Radio Astronomy of the National Academy of Sciences of Ukraine, Kharkiv, Ukraine;
[3]Space Research Centre of Polish Academy of Sciences, Warsaw, Poland.

Strong space weather variations can lead to an effective energy deposit from the solar wind to the Earth's magnetosphere, ionosphere and atmosphere, resulting in the development of geospace storms. During these events, in particular, the ionospheric currents and perturbations in the upper atmosphere are enhanced, the ionospheric disturbances at different Earth's regions are caused. One type of ionospheric perturbations that effectively transfer the storm-driven energy from the auroral region to the middle latitudes and even further to the south are traveling ionospheric disturbances (TIDs). Understanding the generation and propagation of TIDs is essential for predicting and mitigating their effects on communication, navigation, and other technological systems that rely on the ionosphere. Monitoring

space weather variations and their impact on the ionosphere is crucial for maintaining resilience and efficiency of such systems.

The geospace storms caused by different drivers such as coronal mass ejections (CME) and corotating interaction regions (CIR) are known to have quite different effects on the ring current and the auroral activity. Moreover, despite the larger energy output of CME-driven storms, the energy coupling and input are more effective for the geospace storms driven by CIR activities. Storm-time TIDs are usually generated at high latitudes through Joule heating and particle precipitation and propagate mainly southward. The TID intensity at the middle latitudes significantly depends not only from the storm driver, but also from the time of day, season, solar activity, intensity of perturbations and phase of the geospace storm as well as the presence of other sources like tropospheric convention. Thus, the thorough analysis of the mid-latitude TID behavior during the specific geospace storm enable us to collect the observational results for further statistical analysis and better understand and predict TID characteristics during geospace storm period.

The current study is focused on the TID behavior over three Earth's regions – Europe, North America and South Africa – during the CME-driven geospace storm on 27 -28 February 2023 using GNSS and ionosonde measurements. We detected the enhancement in large-scale TID activity over all three regions on 27 February. It is noteworthy that *Kp* index was equal or greater than 5 continuously during 33 hours (from 18 UT on 26 February till 03 UT on 28 February 2023). This led to the occurrence of TIDs over Europe having different energetics and propagation directions during almost the all-daytime period on 27 February 2023. Though the increase in TID intensity was observed in different time intervals over different Earth's regions, the strong CME hitting the Earth near 16 UT on 27 February resulted in simultaneous TID enhancement over all considered regions with delay of 0.5 – 1.5 hours. The periods of predominant TIDs were 55 – 75 min and their horizontal phase velocities fell in the range of 500 – 1500 m/s. Over Europe and North America, the storm-driven TIDs propagated mainly equatorward while their direction was mostly to the South pole over South Africa. In addition, the TIDs caused by the passage of sunrise solar terminator were also observed over Europe during the storm-time period. The ionosonde observations confirmed the presence and intensifications of TIDs detected by GNSS measurements.

HISTORY OF ASTRONOMY

From the history of the astronomical circle of the Kyiv Polytechnic Institute

L. Bakaeva

Boris Paton State Polytechnic Museum National Technical University of Ukraine «Igor Sikorsky Kyiv Polytechnic Institute», Kyiv, Ukraine

Scientific and technical circles played a significant role in the training of highly qualified specialists of the newly created institutes, they were opened in almost all departments. The circles grew and expanded, gained extremely great interest, both from the students' side and from the professor's side, their activities developed in various directions: library, publishing, excursion, museum, lecture, sectional, scientific, etc. The initiators, as a rule, were senior students who felt and understood that the program course did not give them sufficient knowledge of the latest disciplines and information about scientific and technical achievements. The work of the circles was multifaceted. Student interest in collective work, lively exchange of ideas, deepening and dissemination of theoretical and practical knowledge in various fields was awakened. Presentations, discussions, and debates were very popular among the student body, gathering full audiences.

In the conditions of the first Russian revolution, under the influence of the labor movement and revolutionary social democracy, the democratic student body of the KPI also fought against the autocracy. In 1907-1910, the KPI student body actively opposed the new rules on student organizations, the reactionary circular of June 11, 1907, which in point 4 closed the possibility for students to open legal organizations. In order to legalize the organization, it was necessary to submit an application and a Statute for the approval of the Council of the institute, which should describe all types of activities of the organization. Without this procedure, no student organization had the right to conduct anything at the institute.

According to the list of groups and organizations of students of KPI for the period 1902-1911, there are 24 student organizations that were active in the institute. These are circles, sections, societies, communities, mutual aid funds, reading houses, etc. Among them is the Astronomical (physic-astronomical) circle.

Unfortunately, the astronomical circle is represented by a limited number of documents: the Statute and two working letters to the director and the architect of the institute, which does not provide an opportunity to reveal the activities of this circle. We have the following documents: 1.

Form for letters with a stamp of the Astronomical Circle; 2. Seal of the Astronomical Circle; 3. Charter of the student astronomical circle at the Kyiv Polytechnic Institute; 4. A request to the director of the KPI from the Board of the Astronomical Circle dated March 17, 1910, to provide the circle with a tower over the meteorological observatory and speed up the resolution of this issue, since the appearance of Halley's comet requires a place for observations. 5. Letter to the architect of the institute V.A. Obremskyi dated March 30, 1910, with a request to preliminarily inspect the specified tower for safety, which the Authority temporarily granted to the group.

According to the signatures of the letters, it was established that the leader of the circle in 1910 was a student of the mechanical department of the KPI (admitted in 1906) V.V. Iordan, and the secretary was a student of the Mechanical Faculty of KPI (admitted in 1909) B. I. Trautskyi.

We assume that the astronomical circle carried out its activities in the institute legally, since it had a Statute, a seal and its own form for letters. Appeals to the Board and director of the institute are written on these forms. The work of the group was carried out according to its Charter. The statute of the Astronomical Circle is handwritten and consists of seven paragraphs, without date or seal.

Resesarch in the Field of Thermal Physics at KPI and development of Rocket Technology in the 20th Century

L. Bashtova

Boris Paton State Polytechnic Museum National Technical University of Ukraine «Igor Sikorsky Kyiv Polytechnic Institute», Kyiv, Ukraine

In the 40s of the last century there has been a rapid development of energy-intensive technologies with intense thermal processes. At that time, nuclear energy, rocket technology, supersonic aviation, and powerful long-range radio-electronic devices were being created. New technique was characterized by highly concentrated energy flows, which were accompanied by intensive heat release, excess of permissible temperatures and temperature stresses, and the occurrence of instability in highly forced heat exchange systems. High temperature technologies and processes were used to create new devices. These thermophysical problems required theoretical and experimental studies of heat transfer processes under high thermal loads. Such studies were organized in the system of heat and power

engineering institutes of the Academy of Sciences and in scientific laboratories of the largest higher educational institutions of the country.

One of the first to study these processes in Ukraine was a professor at Kyiv Polytechnic Institute (KPI, now KPI named after Ihor Sikorskyi), head of the Department of Boiler Installations (from 1938 to 1965) of the Faculty of Thermal Engineering (TEF), acad. Academy of Sciences of the Ukrainian SSR (1964) - Vsevolod Tolubinskyi (1904 - 1988). The scientist was a specialist in the thermophysics, the author of practical developments in thermal power engineering and industrial heat engineering. He is a laureate of the Prize of the Academy of Sciences of the Ukrainian SSR. G. F. Proskura (1981), which he received for the monograph "Heat Transfer during Boiling".

In the early 1950s, Professor Vsevolod Tolubinskyi, together with the Dean of the TEF A. Ornatsky, created the first specialized laboratory in Ukraine at KPI, which was engaged in the study of highly forced heat transfer and heat exchange crises during the boiling of heat carriers that move, in the conditions when the cooling systems of new equipment work. The heat exchange crisis is a complex phenomenon associated with an abrupt transition from intense bubble boiling to film boiling. This process occurs when an increase in heat input cannot be accompanied by a corresponding increase in heat removal. At the same time, the surface temperature under the film rises sharply. Because of this, there is a loss of structural strength.

In this scientific laboratory of the KPI, research was carried out on behalf of the Institute of Thermal Power Engineering of the Academy of Sciences of Ukraine and enterprises that created new equipment. In 1955, the subject of the TEF heat transfer crisis laboratory was included in the All-Union program of work on cooling liquid-propellant jet engines. Since then, the laboratory has constantly carried out work on orders from design bureaus that developed rocket technology. n 1957, the Problem Laboratory of Heat Transfer and Gas Dynamics was created on its basis. V. Tolubinskyi was appointed its scientific supervisor. He developed a scheme of a unique pilot plant with an experimental steam generator of supercritical steam parameters of 400 atm 700°C and expanded the directions of scientific research. Studies of heat exchange processes in rocket technology for the creation of cooling systems for rocket engines were carried out at KPI until the 1990s. The obtained scientific results were widely used. For example, on their basis, intensive cooling systems were created for powerful radio-electronic generating devices of ultra-high frequencies, rapid-fire artillery systems, etc. The wide range of research of the Problem Laboratory, its scientific connections with industrial enterprises and research institutes

created the conditions for the opening of a new specialty “Thermophysics” at KPI in 1964. In the same year V. Tolubinskyi was appointed to the post of director of the Institute of Technical Thermophysics of the Academy of Sciences of the Ukrainian SSR. , where he continued his research.

A Tireless Observer
(to the 150th anniversary of Sergiy Danylovych Tchorny)

V. Efimenko, L. Kazantseva

Astronomical Observatory of the Taras Shevchenko National University of Kyiv, Ukraine

There are still many inaccuracies and little-known pages in the well-known biography of one of the former directors of the university observatory, Serhiy Danylovych Tchorny. At one time, he worked in many institutions, was an active member of more than one public association, lived in difficult times at the crossroads of eras and political systems, initiated new directions of research and gave rise to many ideas. Using the funds of the Astronomical Museum, archival materials and various printed sources, we expanded the image of this extraordinary personality.

S. D. Tchorny was born on January 24, 1874 in the village of Lebedyne in the former Kyiv province. In 1893, he graduated from the first Kyiv gymnasium and entered Kyiv University at the mathematics department of the physics and mathematics faculty, which he graduated in 1897. After graduating from the university, S.D. Tchorny taught physics and mathematics at the theological seminary in Vologda, at the diocesan women's gymnasium, and worked as a teacher at the Nemyrivskaya gymnasium. In 1990, he returned to Kyiv and began teaching mathematics in the cadet corps, and since 1903 in the second Kyiv gymnasium. In 1906, he received the title of private docent, in 1907 and 1908 he lectured at Kyiv University on theoretical astronomy and celestial mechanics. In 1908, S.D. Black defended his dissertation at St. Petersburg University on the topic "On the number of possible solutions to the problem of calculating parabolic orbits according to the Olbers method", for which he was awarded the degree of Master of Astronomy and Higher Geodesy.

1908 S.D. Tchorny was elected a professor at the University of Warsaw and director of the university's astronomical observatory and meteorological station. In Warsaw, he gives lectures on astronomy and geodesy for students

of the Faculty of Physics and Mathematics, involves them in astronomical observations. In 1915, in connection with the approach of hostilities of the First World War to Warsaw, the university was evacuated to Rostov-on-Don.

In 1923, Kyiv University elected S.D. Tchorny professor of astronomy. At the same time, he was appointed director of the Kyiv Astronomical Observatory, which was going through difficult times at the time. In order to stimulate scientific and teaching activities in the observatory, he contributed in every possible way to the activation of astronomical observations. S.D. Tchorny personally conducted observations at the Mertz refractor, involved all collaborators in this program. During the time of S.D. Tchorny Kyiv Observatory took an active part in the observation of the total solar eclipse on July 19, 1936, observations of changing stars began, and the passage of Mercury across the Sun's disk was successfully observed on May 7, 1924 and November 10, 1927. The observations of sunspots and flares, which S. D. Tchorny started in Rostov. They were new for the Kyiv Observatory, but over time they became one of the main directions of its activity. The results of the observations were elaborated and then published in leading foreign journals: S.D. Tchorny understood the importance of having his own publications for the observatory's prestige and strengthening its contacts with other astronomical institutions. Therefore, with the support of the Academy of Sciences of Ukraine, he renewed the publication of "Annals of the Observatory". In 1937, a graduate school was established at the observatory. The first graduate students of Professor Tchorny were graduates of Kyiv University O.K. Korol and M.M. Astafov. Over time, the former became one of the leading scientists of the GAO of the National Academy of Sciences of Ukraine, the latter died tragically during the war years 1941–1945. S.D. Tchorny combined with a large scientific popularization activity. In 1927, together with I.I. Ilyinskiy and M.O. Rudskiy, he founded the Ukrainian Society of World Studies, which was intensively active until 1935. S.D. Tchorny is the author of the first textbook of descriptive astronomy in the Ukrainian language. This book was written at the level of the achievements in astronomy of those years, is full of information on the history of science astronomy, and is illustrated with photographs, including many photographs of the Kyiv Observatory and its instruments.

In the spring of 1935, the state of health of S.D. Tchorny 's condition worsened, so he stopped lecturing at the university, leaving behind him the management of graduate students and the observatory. In 1939, he appealed to the People's Commissariat of education of Ukraine with a request to release him from the duties of director of the observatory. 1939 Tchorny

S.D. resigns from the university, moves to Kursk and begins a professorship at the Kursk Pedagogical Institute.

On February 11, 1956, his life ended. Memory of S.D. Tchorny as a scientist and researcher will be preserved in his rich theoretical heritage and in the results of his astronomical observations.

Observationj of the August Solar Eclipse of 1914 Based on Archive Materials

L. Kazantseva

Astronomical Museum at the Astronomical Observatory of the Taras Shevchenko National University of Kyiv, Ukraine

The band of visibility of the solar eclipse on August 21, 1914 passed through Ukraine. The scientists of the world were preparing for the observation of this phenomenon in advance for many reasons. The successful placement of the strip on land almost in the centre of Europe, the favourable circumstances of the phenomenon, the appearance of fundamentally new instruments for observation, the opportunity to test new assumptions from Albert Einstein's theory of relativity. At the beginning of summer, expeditions from various countries began to arrive in Ukraine. But the beginning of the First World War forced some to urgently change their plans.

In the stock collections of the Astronomical Museum of the Astronomical Observatory of Taras Shevchenko National University of Kyiv, there are separate materials related to preparation for observations, reception of foreign expeditions, society's reaction to this astronomical phenomenon and educational work with the population, a description of the phenomenon itself and the results of observations.

Additional materials from printed sources and archival institutions expand the information about this extraordinary astronomical event. There are also publications that were prepared by various institutions and organizations on the eve of the phenomenon with detailed information about the circumstances of the event, a zone of sight map. Clippings from various newspapers with information about the arrival of the expeditions, their work and the eclipse itself have been preserved. In addition, there are some memories of the participants of the observations at various points. Using various available publications in scientific journals about this astronomical

phenomenon, archival sources, information from popular science sources and modern sites, you can make a general picture of preparation and observation of a rare astronomical phenomenon in the conditions of the beginning world war.

Academician Mykola Barabashov's Scientific and Organizational Activities

Yu. Koval

National Technical University "Kharkiv Polytechnic Institute", Kharkiv, Ukraine

2024 marks the 130th anniversary of the birth of the outstanding Ukrainian astronomer, planetologist, academician of the Academy of Sciences of the Ukrainian SSR Mykola Barabashov (1894–1971). The scientist dealt with various problems of astrophysics, his main scientific works were devoted to the study of physical conditions on the Moon and the surface of the planets of the Solar System. At the Kharkiv Astronomical Observatory, which Barabashov headed for almost 40 years, he initiated the creation of a scientific school of planetary science, the results of which gained worldwide recognition at the beginning of the space age.

The astronomer was active in the dissemination of astronomical knowledge: even during his student years, he built a private observatory with a dome on the roof of his family house, constructed a small instrument for conducting observations with his own hands; in the 1920s, he compiled programmes and delivered publicly accessible public lectures (received the prize of the People's Commissariat of Education of the Ukrainian SSR for a series of thematic lectures); organized an amateur astronomical club and the "People's Observatory" at the Artem All-Ukrainian Social Museum which played a key role in the development of astronomy in Kharkiv.

Mykola Barabashov was engaged in the construction of new instruments, in particular, on his initiative, a new astrophysical instrument – a spectrohelioscope – was created at the Kharkiv Astronomical Observatory (1935). After its introduction, systematic spectrohelioscopic observations were started in Kharkiv.

Under the general leadership of Mykola Barabashov in the 1930s, the creation of a new Central Ukrainian Observatory was initiated which was supposed to be built on the basis of the Kharkiv Astronomical Observatory. This project remained unrealized for various reasons. The scientist also

promoted the idea of moving the instrument base of the university observatory outside the city in order to solve the problem of improving conditions for astronomical observations.

Mykola Barabashov's activity in implementing various astronomical projects was multifaceted: he proposed the idea of placing astronomical instruments on the roof of the new main building of Kharkiv State University in the 1950s (not implemented); in the same period, he developed a project for the creation of the Institute of Planetary Research in Kharkiv (not implemented); under his leadership, the Chuguyivska (Hrakivska) observation station of the Kharkiv Astronomical Observatory was created (1962).

Barabashov's contribution to the organization of planetary research in astronomical institutions of the USSR is significant. During 1949–1966, he headed the commission on planetary physics created at the Astronomical Council of the Academy of Sciences of the USSR; worked in other commissions of this Council – on the study of the Sun, study of conditions on the Moon and planets, subcommittee on the nature of the lunar surface; was a member of the commission for the physical study of planets and satellites of the International Astronomical Union; from 1952 he headed the Astronomical Committee of the Academy of Sciences of the Ukrainian SSR.

Academician Barabashov launched large-scale activities to hold the International Geophysical Year (1957) and organize observations of the first artificial Earth satellites; on his initiative, planetariums were created in various cities. He became one of the authors and editor of the first "Atlas of the rear side of the Moon" (1960) which was prepared based on photographs obtained by the automatic interplanetary station "Luna-3". Due to the leadership activity of Mykola Barabashov, the Kharkiv Astronomical Observatory became one of the few university observatories in the USSR that took a direct part in the Soviet space programme in the 1960s.

Considering Mykola Barabashov's indisputable contribution to the study of the Moon and the planets of the Solar System, by the decision of the world scientific community, some astronomical objects (an asteroid 2883 in the main belt, a crater on Mars) were named after the astronomer.

Space Research that went down in the History of Ukraine and the World

T. Ozozhenko

Boris Paton State Polytechnic Museum National Technical University of Ukraine «Igor Sikorsky Kyiv Polytechnic Institute», Kyiv, Ukraine

In the early 1960s, the first stages of practical astronautics began. The former USSR and the United States were ahead of other countries in this regard. The first projects of long-lived space orbital stations were already being developed. To create, maintain, and repair them, the idea of welding in space was born, which belonged to Sergei Korolev.

At the first stage, experimental welding equipment was developed for a number of the most promising welding methods in space. Leading scientific institutions of the country conducted relevant research and developed and manufactured a special welding machine “Vulcan” on the basis of the E.O. Paton Institute of Electric Welding.

The first experiments on joining small parts together were performed on October 16, 1969, on the Soyuz-6 spacecraft by cosmonauts G.S. Shonin and V.M. Kubasov. The complex device “Vulcan” allowed to automatically perform work using arc, plasma and electron beam methods.

It was continued to improve welding technologies in interstellar space. In 1979-1984, the E.O. Paton Institute of Electric Welding developed the device “Evaporator”, which allowed conducting experiments on the application and restoration of thin surface metal coatings on samples of structural steels.

The exposition of Borys Paton State Polytechnic Museum presents the “Evaporator-80” unit. This is the “backup” model that was in the Mission Control Center when the analog was used aboard the Salyut-6 orbital station.

Naturally, all instruments for space were made in triplicate. One was used for training on Earth, the second went into space, and the third was a “backup” in case the second one broke down. The “understudy” sample simultaneously performed all the same operations as in the station for providing operational advice.

The Vaporizer-80 unit was used aboard the Salyut-6 space station by cosmonauts V. Ryumin and V. Lyakhov in June 1979. They sprayed silver onto samples of space station materials.

Almost five years after the first experiments, the leading Institute for Electric Welding developed a new welding machine called UHT - a universal handheld tool, based on the first two devices, Vulcan and Isparitel. "UHT" has been welding metal structures perfectly in airless space, space, as well as in zero gravity and aggressive environments. It was also able to weld titanium and perform work in sudden temperature changes. The first tests of the device took place on July 25, 1984, at the Salyut-7 orbital station. For three hours in outer space, Vladimir Dzhanibekov and the first woman to work with him, Svetlana Savitskaya, performed this complex welding task in space.

PolyITAN-1 – the first Ukrainian nanosatellite

A. Seredin

Boris Paton State Polytechnic Museum National Technical University of Ukraine «Igor
Sikorsky Kyiv Polytechnic Institute», Kyiv, Ukraine

Before we start talking about this spacecraft, let's define what we can call a nanosatellite. So, a nanosatellite is a type of artificial Earth satellite that weighs from 1 to 10 kg. The nanosatellites also include artificial satellites of the CubeSat format, which are made in the form of a cube with side dimensions of 10x10x10 cm and weighing up to 1.33 kg. The emergence of artificial Earth satellites with such small size and weight was made possible by the miniaturization of electronic components. The peculiarity of such satellites, in addition to their low weight and size, is that they are manufactured using electronics and software based on off-the-shelf industrial and commercial solutions, which significantly reduces the cost of the nanosatellite and increases its versatility.

The cost of launching a group of nanosatellites into orbit is quite low compared to launching conventional artificial satellites. For example, in 2004, the cost of launching one nanosatellite into orbit was $65-80 thousand, which allows universities to develop such satellites. Nanosatellites are developed both by universities for applied space research and by private companies.

Ukraine did not stand aside from the creation of university nanosatellites. In 2014, a nanosatellite of the Kyiv Polytechnic Institute was launched into orbit - the first Ukrainian nanosatellite of the CubeSat format, which was named PolyITAN-1. This nanosatellite was the first in the line of

nanosatellites developed by Kyiv Polytechnic Institute (several models were produced – PolyITAN-2-SAU, PolyITAN-3-PUT, PolyITAN-4-Plant, PolyITAN-HP-30).

However, let's get back to the first sample of the PolyITAN-1 nanosatellite, the active development of which began back in 2009. A group of young scientists and engineers from different faculties and institutes of Kyiv Polytechnic - the Faculty of Heat and Power Engineering, the Faculty of Radio Engineering, the Faculty of Electronics, and the Institute of Telecommunication Systems - took part in the creation of the nanosatellite. Borys Rassamakin, PhD in Engineering, became the project manager. As mentioned earlier, the PolyITAN-1 nanosatellite is made in the CubeSat format, with dimensions of 10x10x10 cm and a weight of 1 kg. A commercial microcontroller of the Cortex-M3 type was used as the basis of the control system, although in-house components, including solar panels, were also used. The nanosatellite is equipped with: - a data processing subsystem; - an orientation and stabilization subsystem; - a navigation and telemetry subsystem; - a power supply subsystem; - a transmitter subsystem; - a cable network; - a carrier body. As an example of the versatility of such nanosatellites, it is worth noting that all the modules created for this nanosatellite can be used for other models of satellites for various purposes.

The PolyITAN-1 nanosatellite was successfully launched by the Dnipro launch vehicle on June 19, 2014. At the same time, 33 more satellites created by scientists from 17 countries were launched, as well as a platform with QuadPack launch containers developed by ISIS (Delft, the Netherlands), which contained university microsatellites from Argentina, Belgium, Brazil, Denmark, Israel, Singapore, and the United States.

Arithmeter and Astronomy

Yu. Shevela

Astronomical Museum at the Astronomical Observatory of the Taras Shevchenko National University of Kyiv, Ukraine

Astronomy has always required a lot of calculations and has long used special tables and logarithmic rulers to simplify calculations.
At the same time, attempts to automate calculations by famous mathematicians and inventor engineers did not stop, starting from Leonardo

da Vinci's "List Machine" (XVI century) to the "Logical Thinking Machine" of Kharkiv professors P.D. Khrushchev and O.M. Shkukarev (XX century).

For several centuries, inventors searched for the ideal ratio: relative technical ease of manufacture (hence the possibility of serial production), ease of use and accuracy of calculations. The road was long...

Most of these machines were produced in one copy, or remained only in the form of drawings, according to which some were restored in our time as an exhibit for a museum.

Charles-Xavier Thomas de Colmar, founder and head of the Parisian insurance companies "Phoenix" and "Soley", was the first manufacturer of serial calculating machines for performing four arithmetic operations. Their production began in 1821, and these same machines received a permanent name - arithmetic meter (from the Greek arithmos - number and metreo - to measure). Other designers (Arthur Burghardt, J. Edmondson, Ludwig Spitz) improved the arithmetic counter, it was produced in different countries under different names until the beginning of the 20th century. -WITH. Slonimsky, Thomas Hill, Frank Baldwin were not widely distributed, although some of us received the highest awards at world exhibitions.

In 1873, Odner built an arithmetic meter based on Leibniz's machine, but with the use of toothed wheels with a variable number of teeth - "Odner's wheel". The first arithmetic meters in Germany began to be published in 1878, and in 1997, after receiving a German patent for his arithmetic meter (1891), Odner founded his own factory - "Mechanical plant of V.T. Odner", which produces 500 pieces per year. and also in other European countries under different names ("Brunsvig", "Triumphator", etc.). Odner arithmetic meters receive the highest awards at international exhibitions: Chicago (1893), Brussels (1895), Nizhny Novgorod (1896), Stockholm (1897), Paris (1900). After 1917, the plant was confiscated by the new government and closed, Odner's descendants returned to Sweden and founded the company "Original Odner".

An attempt to resume the production of arithmetic meters took place in 1929 at the Dzerzhinsky mechanical plant, and later at the Schetmash plant in Kursk and the Penza computer engineering plant under the name Felix, where they were manufactured almost unchanged until 1978.

In parallel with "Felix", in the 1960s, the "Schetmash" company mastered an improved version of the arithmetic meter with keyboard input of numbers - "VK-1", which is structurally and externally very similar to the Swedish "Facit", and in 70s - "VK-2" where the final operation is already performed by an electric motor (similar to the electromechanical Swedish "Facit"). Another well-known electromechanical arithmetic meter

"Bystrica" is similar to the similar Danish "Contex-10", and "Bystrica-2" to the same Danish "Contex-20".

Foreign electromechanical arithmetic meters were also used: "Archimedes", "Monroe", "Rheinmetal", Zoemtron".

With the development of electrical engineering, the mechanical part of the arithmetic meter was replaced by electronics, and the screen with numbers was replaced by electronic lamps. Such hybrid (lamps + semiconductors) calculators were produced until the mid-1980s (for example, Ros, Iskra).

SUPPLEMENTARY ABSTRACTS

Modeling dusty cometary surface layers of various structures and porosities

V.Reshetnyk[1], I. Lukyanyk[1], Yu.Skorov[2]

[1] Taras Shevchenko National University of Kyiv
[2] University of Braunschweig, Institute for Geophysics and Extraterrestrial Physics

Dust ejection and distant cometary activity - complex problems that cannot be solved with a single line of research, but must be attacked from several directions, which will eventually lead to a consistent solution. We propose the study of dynamical changes in the strength and the possible breakage, due to material fatigue. For this purpose, we simulate various cometary surface layers. The surface layer of comets can be described as an array of dust particles bound together. One of the main characteristics of the near-surface layer structure is porosity. The simplest models of porous media consist of monomer dust particles of the same size. More complex models consider possible heterogeneities and hierarchical structures. In these cases, the size of the monomers, the thickness of the layer and its porosity can vary widely. The gas diffusion through a porous medium obviously depends on its microstructure.

We propose a new approach to generating random porous media with YADE-DEM open-source software, which uses position, orientation, velocity and angular velocity as independent variables of simulated particles which are subject to explicit leapfrog time-integration scheme (Lagrangian method). Our model is based on a specified size distribution of monomer dust particles. We considered power-law, normal, uniform and Weibull distributions for the sizes of the monomers. Such polydisperse models are more representative of the real porous near-surface layers of airless bodies.

We investigated the geometric properties of the generated layers. Distributions of the path lengths of test particles (molecules) in the generated layers were constructed. We also compared the gas permeability through the polidisperse porous layers with the monodisperse layers.

Outburst Parameters Correlations and Analysis of Selected Dwarf Novae

A. Dzygunenko, A. Baransky

Astronomical Observatory, Taras Shevchenko National University of Kyiv, 3 Observatorna St., 04053 Kyiv, Ukraine

We present our research on the correlation analysis of light curves, orbital, and physical parameters of cataclysmic variable stars (CVs), with a particular emphasis on dwarf novae. These are a subclass of CVs, noted for periodic brightness outbursts due to mass transfer from a companion star onto a white dwarf. Our study aimed to thoroughly analyze the physical, orbital, and light curve parameters of five previously unexplored CVs. Additionally, we identified numerous undocumented correlations by conducting a statistical analysis of 653 CVs from the Dwarf Novae Catalog.
The Thermal-Tidal Instability (TTI) model explains cyclical brightening in cataclysmic variable stars through thermal and tidal effects in the accretion disk. We aimed to provide new insights into the correlations between light curve outburst and superoutburst parameters., potentially enhancing or confirming (TTI) model. We analyzed data from the Dwarf Novae Catalog, which includes 653 dwarf novae and 26 parameters, to investigate correlations between superoutburst duration (D_{SO}) and its components (D_P, D_D, D_P). We also examined correlations between the periodicity of the outbursts (P_s, $P_{s\,max}$) and the superoutbursts (P_{sc}, $P_{sc\,max}$).
Specifically focusing on UGSU-type variables, we uncovered significant correlations: superoutburst duration (D_{SO}) with plateau phase duration (D_{SO}) at 0.785 and drop duration (D_D) at 0.771. Using MCMC linear regression ($y = X\beta + \varepsilon$) a Bayesian method, we derived empirical equations for the six strongest correlations identified.
In the second part of our research, we selected five dwarf novae—Gaia21djh, Gaia19bwr, Gaia21akq, Gaia21enu, and Gaia18cjn—and calculated their parameters, including orbital details derived from Lomb-Scargle Periodograms. For UGSU-type variables Gaia21djh, Gaia19bwr, and Gaia21akq, we determined orbital periods: Gaia21djh at approximately 0.0844 days, Gaia19bwr at 0.072 days, and Gaia21akq at 0.09217 days. Further analysis provided period excess ($\varepsilon_{+/-}$) and mass ratio (q):

Gaia21djh showed a period excess of 0.0546 and a mass ratio of 0.2537, Gaia19bwr exhibited a period excess of 0.056 and a mass ratio of 0.258, while Gaia21akq displayed a period excess of 0.05404 and a mass ratio of 0.25085. We also derived masses and radii using empirical equations. Additionally, we calculated parameters of outbursts and superoutbursts for all selected objects using VStar software, and compared our results with existing correlations from the Dwarf Novae Catalog, finding consistent alignment within experimental error margins, confirming the validity of our findings.

In conclusion, our research explores correlations among parameters in cataclysmic variable stars and provides crucial calculations of physical and orbital parameters for selected dwarf novae. These findings offer a fresh perspective on relationships between parameters, potentially advancing our understanding of cataclysmic variable evolution and the (TTI) model, while also uncovering previously unexplored aspects of selected CVs.

Наукове видання

Астрономія та фізика космосу в Київському університеті

в рамках Днів науки в Україні

Міжнародна конференція

м. Київ, 28 – 31 травня 2024 р.

Збірка тез доповідей